University of New South Wales

Sydney, Australia, 2052

Honours Thesis, Semester 1 2014

Bound States of Triplons as an Avenue Toward Spin Liquids

Author:
Bryce Lackenby

Supervisor:
Prof. Oleg Sushkov

June 19, 2014

Abstract

In the antiferromagnetic (AFM) bilayer model the quantum phase transition (QPT) between the ordered state and the disordered state is driven by a spin coupling tuning parameter for nearest neighbour interaction on the lattice. In this thesis, using a bond operator approach, we find the dispersion relation for the triplon quasi-particle deep in the disordered phase. Using this dispersion we find the scattering amplitude of two triplons in the disordered phase and find the bound state and its dependence on the lattice for the different spin channels. We find that the singlet channel ($S = 0$) is the most favourable bound state in this model.

Contents

List of Figures

Acknowledgments

I would like to thank Professor Oleg Sushkov for introducing me to this problem and his continued guidance, help and patience during the past 12 months. The time spent working with Oleg this semester was invaluable and he has my deepest gratitude. I would also like to thank my peers for making it an enjoyable semester.

Note on nomenclature and unit convention

The nomenclature in the field of quantum magnetism has no strict convention. Therefore in this paper I will stick to the convention that spin-waves in the Néel ordered phase are known as "classical spin waves" and the spin-waves in the disordered state are known as triplons (the major focus of this thesis). In the literature triplons are often referred to as magnons although classical spin waves are also magnons.

I will approach the scattering and bound state problem primarily with Feynman diagrams as I feel it conveys the principles clearly, however these diagrams will be accompanied with their mathematical equivalents for the actual computation.

For the 2D bilayer and tripon bound state in chapter 3 we will assume that the lattice spacing is unity for simplicity. However for arbitrary lattice spacing these can easily be restored using dimensional analysis. Also although the number of lattice points N is important in all calculations their dependence cancels in all cases and therefore is omitted.

Introduction

The core of condensed matter physics is the study of different phases of matter, their properties and the transitions between them. Early in the field, these phases were common and ubiquitous in nature such as solids liquids and gases. In the 20th century many more exotic phases of matter emerged and the field rapidly expanded and continues to grow today, especially with the advent of quantum computing. These new exotic phases included the quantum liquid phases such as the superfluid helium state [1] and Bose Einstein condensation (BEC) [2, 3], and perhaps the most paradigm shifting discovery was that of superconductivity [4]. Another major step in condensed matter physics was the leap from classical magnetism and to quantum magnetism. For centuries magnetism was understood in the scope of classical physics through its macroscopic properties, however deeper study into the microscopic theory of magnetism revealed that magnetism was inherently a quantum phenomena and a consequence of the exchange interaction which arises from the properties of quantum statistics and it was simultaneously derived by both Dirac and Heisenberg [5]. Since then a major part of the condensed matter field is the study of these quantum properties of magnetism and is incredibly active today especially in the context of quantum phase transitions (QPTs), BEC of spin waves and superconductivity.

In this thesis I give a brief introduction to the theory of quantum magnetism, spin waves and QPTs before introducing the antiferromagnetic (AFM) bilayer model, which will be considered for the remainder of the thesis. I will demonstrate the quantum criticality of the model and find the dispersion relation for the triplon quasi-particles on the bilayer. Then considering the scattering of two triplons I will derive the bound state between them for a variety of cases.

In essence, the aim of this thesis is to demonstrate the importance of QPTs and the presence of magnetic quasi-particles within the AFM bilayer model and how these quasi-particles interact and form a bound state. This research will ultimately lead to further research on the condensation of these quasi-particles in the AFM bilayer which is an avenue for the much sought after spin liquid.

Importance of this Research

As stated above two major leaps in physics, particularly condensed matter, are the microscopic theories of superconductivity and quantum magnetism and recently there has been increased effort to find a link between the two phenomena. Although the BCS theory of superconductivity has been extremely successful in describing and predicting properties of the superconducting state in conventional low temperature superconductors, a complete description of high temperature superconductivity (HTSC) (which cannot been accurately described by BCS theory) has eluded physicists for almost three decades since their discovery in 1986 [6] in which the 1987 Nobel Prize in physics was awarded for the discovery [7]. These HTSCs are typically cuprates however iron-based HTSC have recently been discovered [8, 9].

In 1987 it was proposed that HTSC could be related to quantum spin liquid phase of an AFM system by Nobel Laureate Philip W. Anderson as there are similarities between the condensation of spin quasi-particles in a quantum spin liquid and the condensation of Cooper pairs in the standard BCS theory[10]. Due to this proposition the study of bound states manifesting in quantum magnetic systems has become extremely topical in the last decade and has manifested in high impacts articles such as [11]. Further information on the connection between spin liquids and HTSC can be found in [12].

Quantum spin liquids were first proposed in 1973 by P.W. Anderson in [13] as a new AFM state as an alternative to the standard Néel state. It was later characterised a disordered state with coupled spins and a non magnetic ground state and therefore an obvious candidate is the disordered regime of the AFM state. A mathematical approach to spin liquids can be found in [14] however the general properties that a spin liquid must display are disorder and display some hydrodynamic variable.

In the context of this thesis we develop the basis of a spin liquid state for a two dimensional frustrated square lattice. We find the bound state of the triplon quasi-particles in the highly disorder regime at absolute zero. This will lead onto important further research particularly in the direction of the condensation of these bounds states and therefore the manifestation a spin liquid in the system.

Thesis Outline

This thesis will progress as follows.

Chapter 1: Introductory Material This chapter contains necessary information required to understand further concepts in the thesis. This includes a brief introduction to quantum magnetism and a further section specifically on the antiferromagnetic state and its relevant properties. Then there will be a brief overview of symmetry considerations in magnetic systems and is finalised by the concept of quasi-particles and how they appear in the context of quantum magnetism.

Chapter 2: Quantum Criticality This chapter will introduce the AFM bilayer model which we will use for the remainder of the thesis. In this we will show the QPT of the bilayer driven by the coupling tuning parameter and find the dispersion relation of triplons traveling through the lattice. We will finish this chapter by giving an overview of previous literature on the bilayer and properties of its QPT.

Chapter 3: Triplon Bound States This is the major work of the thesis where we find the bound states of two triplons travelling through the lattice with an additional frustrated term in the AFM bilayer. We begin by introducing the Bethe-Salpeter equation for a bound state in scattering theory and then apply it to the different spin channels of the bound states and use numerical methods to quantify the bound states.

Chapter 4: Conclusion This is the final chapter where we review the work done in the thesis and present avenues for further research.

Appendix A: Boson Commutation Relations Here we present a brief overview of bosonic commutations and the Bogoliubov transform.

Appendix B: Heisenberg to Bond Operators Calculation This appendix describes how to perfectly map the Heisenberg Hamiltonian to an effective triplon excitation Hamiltonian in a bond operator approach. This technique is applied in chapters 2 and 3.

Appendix C: Spin Scattering Channels This appendix describes the properties of the three bound state spin channels required for the calculations in chapter 3.

Appendix D: Numerical Calculations This is a brief appendix which describes how the summations in chapter 3 were calculated. Sample code is provided for the singlet bound state energy vs coupling constant.

Chapter 1

Introductory Material

1.1 Quantum Magnetism

Magnetism has been a known natural phenomena since ancient times due to it's perculiar properties of attraction and repulsion. These macroscopic properties of magnets have been applied over the centuries to the benefit and progress of humanity in the context of scientific research and engineering. However since the birth of quantum mechanics the the understanding of microscopic properties of magnetism in particular has been an important development modern physics.

The quantum mechanical origin of magnetism is due to the exchange interaction which is a consequence of Fermi-statistics, indistinguisability of electrons and the anti-symmetric requirement of the electron (fermion) wavefunctions. In materials, the macroscopic magnetism arises from the collective alignment of spin of atoms in the materials lattice. These individual spins produce a magnetic moment which causes each atom to act like a small magnet and when a statistically significant amount of these magnetic moments align, the material macroscopically behaves like a magnet. This phenomena is known as ferromagnetism (FM) and is a purely quantum mechanical phenomena and arises purely from the exchange interaction. Another type of magnetism (AFM), the focus of this thesis, is another major area of study in condensed matter physics due to it's exotic properties. Unlike FM described above AFM materials are those where the spins are anti-aligned along the lattice. These two types of magnetism are illustrated in Figure 1.1 and properties of the AFM state will be discussed in detail below.

These quantum magnetic systems are many body systems the models which de-

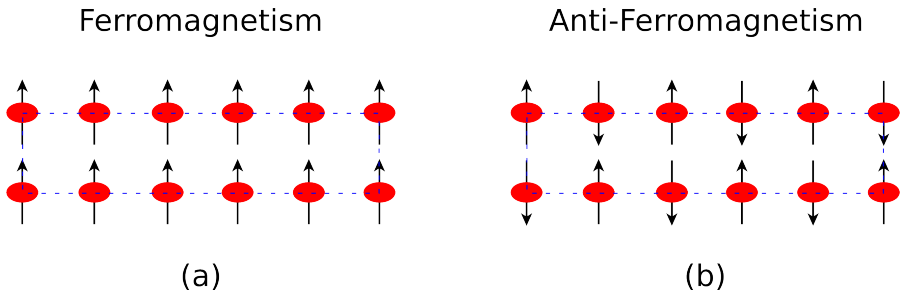

Figure 1.1: Comparison of ordered FM (a) and AFM (b) spin orientation. In the case of FM the spins are all aligned in the same direction, whereas in the AFM case the spins are anti-aligned.

scribe them are non trivial and often approximations. The early models of magnetism only described the FM state and focus on the magnetic susceptibility of the systems and describes average energies and spin expectation values [15, 16]. Though a good basis for quantum magnetism, these models provide only superficial insight into the actual quantum mechanical dynamics of the systems including spin correlations and quantum fluctuations in the lattice [15]. An example of these early models is the Ising model which which describes the interaction of discreet spin operators (either spin up or spin down) in the lattice which interact with neighbouring spins. A great review of this model in the context of FM and its importance and historical implications can be found in [17]. The model we use in this thesis is known as the Heisenberg model,which is a purely quantum mechanical model.

In FM materials the spins of the atoms are aligned in the same direction (Figure 1.1a) in a lattice. In Heisenberg notation the Hamiltonian of the ferromagnetic coupling between lattice points i and j is given by,

$$H_{FM} = -J \sum_{i,j} S_i \cdot S_j, \tag{1.1}$$

Where $J > 0$.

Where S_i is the spin on the ith lattice site.

AFM materials are those which have anti-aligned spins (Figure 1.1b). In Heisenberg

notation the Hamiltonian of the AFM coupling between lattice sites i and j is,

$$H_{AFM} = J \sum_{i,j} S_i \cdot S_j, \tag{1.2}$$

Where $J > 0$.

Contemporary research in quantum magnetism primarily focuses on the study of QPTs, condensed states and their quasi-particles. These require more complicated approaches than the standard Heisenberg or Ising approach and require a field theory approach.

1.2 Properties of the Anti-Ferromagnetic State

As described above the AFM state is one where the anti-alignment of spins is favoured and can be described by the Hamiltonian in 1.2 and pictured in Figure 1.1(a). For simplicity we typically consider this state to be the sum of nearest neighbours only ($\langle i, j \rangle$). Unlike the FM state where the net alignment of spins produces macroscopic magnetic field there will be no net magnetisation for the AFM ground state and therefore there is no macroscopic magnetism. Therefore to study the AFM state we have to use more complex methods such as neutron diffraction [18, 19, 20].

The major property of the FM state is the spontaneous magnetism at the Curie point. The phase below this point is known as the Curie Phase and is characterised by the spontaneous total alignment of spins of the system whereas above the Curie point there still exists ferromagnetic coupling but no net alignment of spins (paramagnetic). The Curie phase is known as the ordered phase of the FM and the phase above the Curie point is known as the disordered phase. In AFM systems there are analogs to these phases. The ordered phase of an AFM system is known as the Néel phase where the anti-aligned spins spontaneously align (similar to the Curie phase but no net magnetisation) and there exists a disordered phase where there is no net polarisation and the AFM ground state can be described by localised singlets known as singlet dimers. In this respect the major difference between the AFM and FM system is what drives this phase transition. In a FM system the phase transition is driven by temperature however in an AFM system there is a phase transition occurs at absolute zero and therefore driven by some other parameter. These phases transitions at absolute zero are the result of quantum fluctuations and are known as QPTs. How these QPTs manifest in the AFM bilayer model will be discussed in chapter 2.

Since the 1930s restrictions to the existence of ordered quantum magnetic states has been studied. It was found that there can be no long range order in crystalline structures for one- or two-dimensional systems [21, 22].

The principle requirement for an AFM is one that is can be characterised by (1.2) and therefore many different lattice structures have been studied which display this property. In this thesis we consider the AFM bilayer (Illustrated in Figure 2.1) which has nearest neighbour interactions on a simple square lattice and in chapter 3 we introduce an additional frustrated coupling to facilitate the calculation.

1.3 Symmetry Breaking in Magnetic Systems

As stated in the previous section, magnetism is the result of a collective alignment or anti-alignment of spins in a particular polarisation. Therefore for magnetisation to occur the spins must "choose" a polarisation despite all polarisations being degenerate. Therefore it has broken rotational symmetry (O(3) symmetry). Also considering the Hamiltonians (1.1) and (1.2) we see there is no term in the Hamiltonian which influences the polarisation of the state and therefore the symmetry is said the be spontaneously broken [23]. Magnetism is the most common example of the spontaneous symmetry breaking as it illustrates it perfectly in that the system arbitrarily "selects" a ground state in a particular direction despite the ground state being infinitely degenerate. This property of is responsible for many of the interesting properties of magnetic materials.

This argument describes how the symmetry is spontaneously broken in the ordered phase of the magnetic materials. In these ordered phases there the phase exhibits long range order which is not present in the disordered phase. In these phases the spontaneously broken symmetry results in what is known as a Goldstone mode[24] in quantum field theory and these Goldstone modes have a gapless dispersion relation as we will show in chapter 2.

However as we will show the disordered phase will have a gapped dispersion relation (also known as a spin gap in this context) for its quasi-particle excitations which is what gives the phase its interesting properties particularly in the context of spin-liquids.

1.4 Quasi-Particles, Spin Waves and Triplons

In condensed matter physics elementary excitations of the system result in a perturbation of the system. These excitations can be modeled as particles which propogate through the system and have definite momenta and energy despite not be directly attributable with discreet elements of the system. These quasi particles are important as they allow us to describe the properties of the excitations through a dispersion relation[25].

Consider the ordered FM and AFM models which have an ordered ground state of parallel and anti-parallel spins respectively. What happens if one of the spins is perturbed in the lattice? By the exchange interaction the perturbed spin will effect it's neighbours spins and this perturbation will propagate throughout the lattice. This propagation through the lattice is known as a spin-wave and are a crucial concept in quantum magnetism as they represent how an excited state translates through the system[15, 26].

The spin waves described above are known as "classical spin waves" and occur in ordered FM and AFM systems [27]. However in the AFM disordered phase (chapter 2) we have to consider a new type of spin wave, a triplon. Unlike the AFM ordered phase where a perturbation or excitation causes a perturbation to the singlet state in a lattice, deep within the disordered phase each dimer is highly localised and therefore an excitation cause the spin of one site to flip creating a "triplet state". This "triplet state" propogates through the lattice like a spin-wave and is a quasi-particle known as a triplon which is illustrated in Figure 1.2. We will elaborate on this concept in chapter 2 with a mathematical basis.

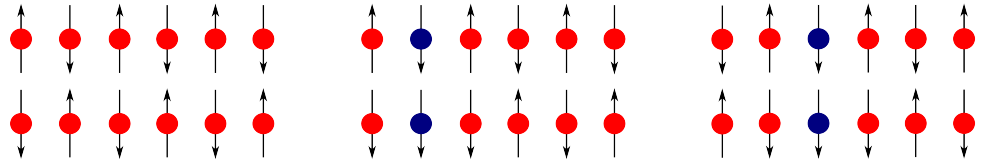

(a) AFM Ground State (b) Excitation of Triplet Pair (c) Propogation of Triplet Pair (Triplon)

Figure 1.2: Idealised illustration of triplon production in AFM ground state. From the simple AFM ground state (a) there is quantum fluctuation which cause the spin to flip at a site producing a triplet (b)(denoted by blue sites). This triplet state propogates along the lattice (c) and acts as a quasi-particle, that is, a triplon.

Chapter 2

Quantum Criticality

A large field of condensed matter physics is the study of QPTs. These are phase transitions of the ground state of the system and therefore occur only at $T = 0K$ and therefore are not thermodynamically dependent and are related to the quantum correlations of the system and the effects of quantum fluctuations. To drive these QPTs we need some sort of tuning parameter g at $T = 0K$ where the QPT occurs for some critical value of the parameter g_c. In this thesis we consider the tuning parameter to be the ratio of the inter- and intra-layer coupling, however there exists other possible tuning parameters for phase transitions such as pressure, electro-magnetic field strength or electron density. A tuning parameter need only influence the quantum correlations in the system to produce a QPT.

For each QPT there exists a Quantum Critical Point (QCP) at some g_c where the phase changes. The study of this critical point gives core information about the behaviour and properties of systems under specific conditions. In the context of the anti-ferromagnetic bilayer with coupling constant tuning parameter the QCP obey the Non-linear $\boldsymbol{\sigma}$ model[28, 29].

A good overview of QPT can be found in the book "Quantum Phase Transitions" by S. Sachdev [30] and for quantum criticality in magnetic systems specifically "Quantum Criticality" by S. Sachdev and B. Keimer [31]. By definition each side of these critical points has a distinct phase, in magnetic media these phases can be catagorised as either ordered or disordered. The ordered phase displays long range order such as the ferromagnetic Curie phase where all the spins are aligned, or the AFM Néel phase where all the spins are antialigned along the lattice. The disordered or dimer phase

does not display this long range order but exhibits the magnetic property localised throughout the lattice for example a paramagnetic state [31]. These localised points are known as dimers in the AFM case. In this thesis we consider a system deep in the disordered phase far away from the critical point.

In this chapter we will discuss the Mermin-Wagner theorem, the Hamiltonian and quantum critical point of the AFM bilayer system including the quasi-particle bandgap. We will also briefly mention previous numerical models and experimental observations of this system in the literature.

2.1 Mermin-Wagner Theorem

The Mermin-Wagner theorem presents a powerful fundamental argument which provides constraints on the existence of phase changes and critical points in magnetic materials [32]. In simple terms, the Mermin Wagner theorem states that at any non zero temperature, a one- or two-dimensional Heisenberg magnetic system with a finite range interaction cannot display long range order (ordered phase in AFM or FM materials) due to thermal fluctuations destroying the order. This means that a phase transition to a magnetic state can only occur at $T = 0K$ for one- and two-dimensional system, although there are no restrictions to three-dimensional systems.

Also AFM materials present another constraint, like thermal fluctations destroying the long range order in one- and two-dimensions. AFM materials have the condition that even at absolute zero there cannot be long range order in one-dimensional systems as quantum fluctuations destroy the order [33, 34]. Therefore the quantum criticality of the AFM ground state can not be studied for a linear chain of spins. In this thesis we study the AFM bilayer and therefore to study the quantum criticality we consider the system at absolute zero where there will be a QPT between the ordered Néel phase and the disordered phase.

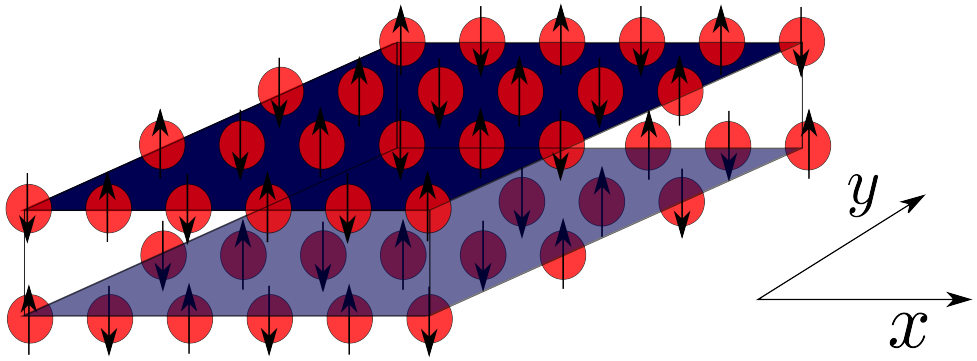

Figure 2.1: Idealised illustration of the AFM bilayer in the ground state.

2.2 Antiferromagnet Bilayer Model and Bond Operators

In this section we consider the unfrustrated antiferromagnetic bilayer [29, 35, 36, 37] shown in Figure 2.1. The Hamiltonian for this model is,

$$H = J_{\parallel} \sum_{\langle i,j \rangle} (\mathbf{S}_{1,i} \cdot \mathbf{S}_{1,j} + \mathbf{S}_{2,i} \cdot \mathbf{S}_{2,j}) + J_{\perp} \sum_{i} \mathbf{S}_{1,i} \cdot \mathbf{S}_{2,i}. \tag{2.1}$$

Where $J_{\parallel}$ is the intra-layer spin coupling and $J_{\perp}$ is the inter-layer spin coupling and they are both positive. $\mathbf{S}$ are spin operators which have magnitude $S = \frac{1}{2}$ and therefore belong to the SU(2) group, and the subscripts denotes their position on the bilayer. The first subscript is if it is on the first (1) or second (2) layer and the second subscript is their fixed position along the layer. Eg. $\mathbf{S}_{1,i}$ is spin on the first layer at position i. The summation over $\langle i, j \rangle$ is the sum over nearest neighbours. Therefore the first two terms in the Hamiltonian represent the interaction between adjacent spins on the same layer and the third term is the magnetic coupling between the same site on each layer.

We now define singlet and triplet description for inter-layer pairs. This splitting of the layers into pairs is known as dimerisation where each pair is a dimer (Figure 2.2)[38]. We define these dimers using the bond operators in the mean-field approach of S. Sachdev and R. N. Bhatt[39]. There are 3 possible triplet dimer excitations for each polarisation and one singlet dimer (a system with only singlet dimers represents the ground state of the system).

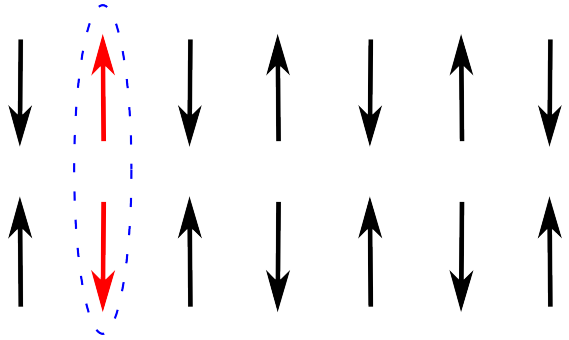

Figure 2.2: Representation of a dimer in the disordered phase of AFM chain. The dashed blue oval enclosing the two red spins is a dimer, in this case the dimer is a singlet. (Idealisation, the dimer state does not exhibit the Néel order shown.)

$$\begin{aligned}
\text{Singlet dimer:}\quad |s\rangle = s^\dagger |0\rangle &= \frac{1}{\sqrt{2}}\left(|\uparrow\downarrow\rangle - |\downarrow\uparrow\rangle\right) \\
\text{Triplet dimers:}\quad |t_x\rangle = t_x^\dagger |0\rangle &= -\frac{1}{\sqrt{2}}\left(|\uparrow\uparrow\rangle - |\downarrow\downarrow\rangle\right) \\
|t_y\rangle = t_y^\dagger |0\rangle &= \frac{i}{\sqrt{2}}\left(|\uparrow\uparrow\rangle + |\downarrow\downarrow\rangle\right) \\
|t_z\rangle = t_x^\dagger |0\rangle &= \frac{1}{\sqrt{2}}\left(|\uparrow\downarrow\rangle + |\downarrow\uparrow\rangle\right)
\end{aligned} \tag{2.2}$$

In a mean field theory the spin of the particle can be represented as $\mathbf{S}_i = \frac{\hbar}{2} a^\dagger_{i\mu} \hat{\boldsymbol{\sigma}}_{\mu\nu} a_{i\nu}$ were $\hat{\boldsymbol{\sigma}}$ are the Pauli matrices and $a^\dagger$ and a are spinor creation and annihilation operator respectively. Using this, the spins can be written in operator form using 2.2 and finding all the matrix elements of the transform that the spins of the dimers can be represented by [39]:

$$\begin{aligned}
S_{1,\alpha} &= \frac{1}{2}\left(s^\dagger t_\alpha + t_\alpha^\dagger s - i\epsilon_{\alpha\beta\gamma} t_\beta^\dagger t_\gamma\right), \\
S_{2,\alpha} &= -\frac{1}{2}\left(s^\dagger t_\alpha + t_\alpha^\dagger s + i\epsilon_{\alpha\beta\gamma} t_\beta^\dagger t_\gamma\right).
\end{aligned} \tag{2.3}$$

Where ϵ is the totally antisymmetric tensor and $\alpha = x, y, z$.

To employ this operator method certain constraints need to be applied. For each dimer we can only have a single bond, ie. either a singlet or one of the triplets. Therefore for

each site dimer in the bilayer there is the operator hardcore constraint,

$$s^\dagger s + t_\alpha^\dagger t_\alpha = 1. \tag{2.4}$$

It should be noted that these operators satisfy the bosonic commutator relations (Appendix A). The spin states represented above display properties of spin SU(2) operators and can generate O(4) rotations in space[39].

2.3 Effective Hamiltonian

Using this new basis, we can construct and effective Hamiltonian by perfectly mapping the new spin operators (2.3) to the Heisenberg Hamiltonian (2.1) this is shown explicitly in Appendix B. The effective Hamiltonian becomes [40],

$$\begin{aligned}
H_{eff} &= H_2 + H_3 + H_4 \\
\text{Where } H_2 &= \sum_{\mathbf{k},\alpha} \left\{ A_\mathbf{k} t_{\mathbf{k}\alpha}^\dagger t_{\mathbf{k}\alpha} + \frac{B_\mathbf{k}}{2} \left(t_{\mathbf{k},\alpha}^\dagger t_{\mathbf{k}\alpha}^\dagger + t_{\mathbf{k}\alpha} t_{\mathbf{k}\alpha} \right) \right\}, \\
H_3 &= 0, \\
H_4 &= \frac{J_\parallel}{2} \sum_{<i,j>} \left[t_{\alpha i}^\dagger t_{\beta j}^\dagger t_{\beta i} t_{\alpha j} - t_{\alpha i}^\dagger t_{\alpha j}^\dagger t_{\beta i} t_{\beta j} \right], \\
H_C &= U \sum_{i,\alpha\beta} t_{\alpha i}^\dagger t_{\beta i}^\dagger t_{\beta i} t_{\alpha i} \ , U \to \infty, \\
\text{Where } A_\mathbf{k} &= J_\perp + 2J_\parallel \xi_k, \\
B_\mathbf{k} &= 2J_\parallel \xi_\mathbf{k}, \\
\xi_\mathbf{k} &= \frac{1}{2} \left(\cos(k_x) + \cos k_y \right).
\end{aligned} \tag{2.5}$$

Where the elements of H_2 have been transformed to momentum space using the Fourier transform,

$$t_{\alpha,i} = \frac{1}{\sqrt{N}} \sum_i e^{i(ki)} t_{\alpha,k}. \tag{2.6}$$

Where N is a normalisation term due the number of lattice points, we ignore this from here on.

Interestingly, the only term dependent on the interlayer coupling is the second order term. This will become apparent in the next section where we will see that the

quantum critical point is proportional to this coupling. However the higher order terms represent the production of multiple triplons in the system. H_4 represents the production of two adjacent triplons which will be the focus of our bound state in chapter 3.

The hardcore repulsion term H_c and enforces (2.4) which means that two triplons cannot exist on the same site.

2.4 Quasi-particle Band gap

To find the quasi-particle band gap we assume that only the second order excitations (2.5) influence the band gap and all higher order terms have a negligible impact [40]. To find this band gap we use the method of Bogoliubov [41, 42]. First we find the the Bogoliubov transform for the momentum dependent operators. Letting β be the Bogoliubov quasi-particles and suppressing spin notation we have,

$$t_{\mathbf{k}} = u_{\mathbf{k}}\beta_{\mathbf{k}} + v_{\mathbf{k}}\beta^{\dagger}_{-\mathbf{k}},$$
$$t^{\dagger}_{\mathbf{k}} = u_{\mathbf{k}}\beta^{\dagger}_{\mathbf{k}} + v_{\mathbf{k}}\beta_{-\mathbf{k}}.$$

Substituting these into H_2 we find that,

$$H_2 = \sum_{\mathbf{k}} A_{\mathbf{k}}\left(u^2_{\mathbf{k}} + v^2_{\mathbf{k}}\right)\beta^{\dagger}_{-\mathbf{k}}\beta_{-\mathbf{k}} + A_{\mathbf{k}}u_{\mathbf{k}}v_{\mathbf{k}}\left(\beta^{\dagger}_{-\mathbf{k}}\beta^{\dagger}_{\mathbf{k}} + \beta_{-\mathbf{k}}\beta_{\mathbf{k}}\right) + \quad (2.7)$$
$$\frac{B_{\mathbf{k}}}{2}u_{\mathbf{k}}v_{\mathbf{k}}\left(\beta^{\dagger}_{\mathbf{k}}\beta_{\mathbf{k}} + \beta^{\dagger}_{-\mathbf{k}}\beta_{-\mathbf{k}}\right) + \frac{B_{\mathbf{k}}}{2}\left[u^2_{\mathbf{k}}\left(\beta^{\dagger}_{\mathbf{k}}\beta^{\dagger}_{-\mathbf{k}} + \beta_{\mathbf{k}}\beta_{-\mathbf{k}}\right) + v^2_{\mathbf{k}}\left(\beta_{-\mathbf{k}} + \beta_{\mathbf{k}}\beta^{\dagger}_{-\mathbf{k}}\beta^{\dagger}_{\mathbf{k}}\right)\right].$$

The excitation spectrum is given by the coefficient of the number of quasi-particle excitations, that is $\omega_{\mathbf{k}}n_{\beta}$ where the number of excitation are terms with the form,

$$n_{\beta} = \beta^{\dagger}\beta.$$

Therefore we have to set the coefficients for all other terms (those of the form $\beta\beta$ and $\beta^{\dagger}\beta^{\dagger}$) to 0 which gives the condition,

$$A_{\mathbf{k}}u_{\mathbf{k}}v_{\mathbf{k}} + B_{\mathbf{k}}\left(u^2_{\mathbf{k}} + v^2_{\mathbf{k}}\right) = 0.$$

Therefore comparing the remainder of the terms in (2.7) with $\omega_{\mathbf{k}} n_\beta$ leaves us with the equation,

$$\omega_{\mathbf{k}} = \sum_{\mathbf{k}} A_{\mathbf{k}} \left(u_{\mathbf{k}}^2 + v_{\mathbf{k}}^2 \right) + B_{\mathbf{k}} u_{\mathbf{k}} v_{\mathbf{k}}.$$

Now using the commutation relation of the bosonic Bogoliubov transformation,

$$\begin{aligned} u_{\mathbf{k}}^2 - v_{\mathbf{k}}^2 &= 1, \\ \Rightarrow u_{\mathbf{k}} &= \cosh(\theta), \\ v_{\mathbf{k}} &= \sinh(\theta). \end{aligned}$$

We solve the self consistent equation and find that the bandgap is given by,

$$\begin{aligned} \omega_{\mathbf{k}}^2 &= A_{\mathbf{k}} - B_{\mathbf{k}}, \\ \Rightarrow \omega_{\mathbf{k}} &= \sqrt{J_\perp^2 + 4 J_\parallel J_\perp \xi_{\mathbf{k}}}, \\ \Rightarrow \frac{\omega_{\mathbf{k}}}{J_\perp} &= \sqrt{1 + \frac{4 J_\parallel}{J_\perp} \xi_{\mathbf{k}}}. \end{aligned} \tag{2.8}$$

This is the excitation spectrum for the AFM bilayer. From this we can see that there is a quantum critical point where band gap vanishes and there is a minimum in the dispersion which corresponds to,

$$\begin{aligned} \omega_{\mathbf{k}} = 0 \Rightarrow J_\perp^2 + 4 J_\parallel J_\perp \xi_{\mathbf{k}} &= 0, \\ \Rightarrow \frac{J_\perp}{J_\parallel} &= -4 \xi_{\mathbf{k}} = J_c, \\ \Rightarrow J_c &= 4 \text{ for } \xi_{\mathbf{k}} = -1. \end{aligned} \tag{2.9}$$

However this is an extremely crude approximation to the QCP as it does not account for correlations between spins in the system. We will present a more accurate value below.

This QCP shows that in the ordered phase ($\frac{J_\perp}{J_\parallel} < J_c$) we have a Goldstone boson (gapless dispersion, $\omega_{\mathbf{k}} = 0$ for $\mathbf{q} \to 0$) and it the disordered phase the triplon excitations are gapped ($\omega_{\mathbf{k}} \neq 0$). This represents the phase transition between the Néel ordered phase and the disordered phase ($\frac{J_\perp}{J_\parallel} > J_c$). In this thesis we consider the regime deep in the disordered domain ($J_\perp \gg J_\parallel$) which intuitively corresponds to interlayer sites highly correlated with little effect on adjacent sites in comparison. We can safely

catagorise the lattice sights as dimers. Therefore in this regime we can take the the first order approximation of the quasi-particle excitation spectrum as,

$$\begin{aligned} \omega_{\mathbf{k}}^2 &= \sqrt{J^2\perp + 4J_{\parallel}J_{\perp}\xi\mathbf{k}}, \\ \Rightarrow \omega_{\mathbf{k}} &\approx J_{\perp} + 2J_{\parallel}\xi_{\mathbf{k}}. \end{aligned} \tag{2.10}$$

2.5 Quantum Critical Point and Spin Gap

In this section I will give brief overview on the literature related to the quantum criticality of the AFM bilayer. The minimum of the non zero excitation spectrum is also known as the spin gap [38, 43] or triplet gap as it is the minimum required energy need to flip the total spin of the dimer. As we can see from (2.8) the minimum will occur at $\mathbf{q} = (\pi, \pi)$ and therefore we define the spin gap dispersion to be $\Delta = \omega_{\pi,\pi}$[40]. The dispersion relation given by (2.8) has been solved numerically to find the QCP and the spin gap in the disordered phase in [40]. In this paper they find that the QCP is found at $\frac{J_{\perp}}{J_{\parallel}} \approx 2.57$ (Figure 2.3). Also as we are considering a two-dimensional system we also have a high dependence on the direction of propogation for the triplons. In Figure 2.4 from [40] the triplet dispersion is show for the spectrum of momentum within the Brillouin zone of the square lattice and we can see a clear minimum at $\mathbf{q} = (\pi, \pi)$. Although this is the dispersion around the QCP ($\frac{J_{\perp}}{J_{\parallel}} \approx 2.57$) and for the bound states we are considering the highly disordered regime ($J_{\perp} \gg J_{\parallel}$) we will have to consider the minimum of the excitation spectrum.

Experimentally the AFM Bilayer is an important model for the properties of antiferromagnetism. As stated above the spin gap is thought to be an integral part of high temperature superconductivity. The bilayer model has physical implications as it is thought to be a good model for many of the cuprates [44, 45, 46]

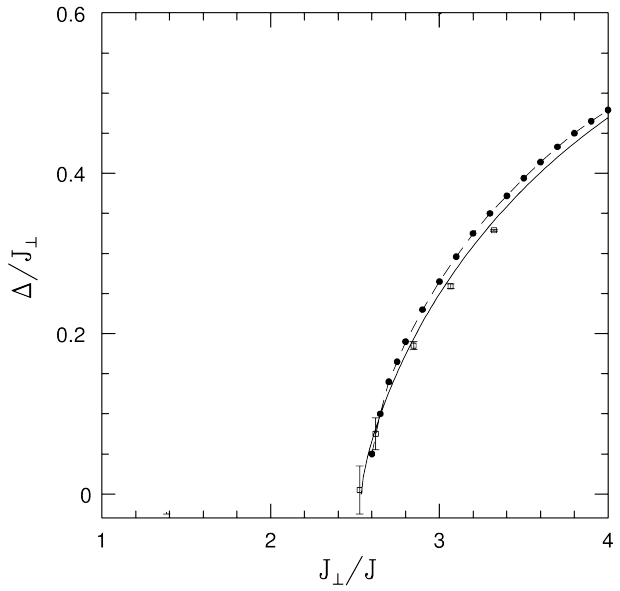

Figure 2.3: ("Novel Approach to Description of Spin Liquid Phases in Low Dimensional Quamtum Antiferromagnets", V. Kotov *et al.*, PRL, vol. **80** 26) This shows the numerical spin gap for the QAFM bilayer. This plot shows a numerical plot of the dispersion relation in an AFM bilayer including spin correlations not considered in our calculation. The different types of lines used denote different approximations and solutions to the series however for the purpose of this discussion we only note the critical coupling at $\frac{J_\perp}{J_\parallel} \approx 2.57$ and the gapless dispersion below this point.

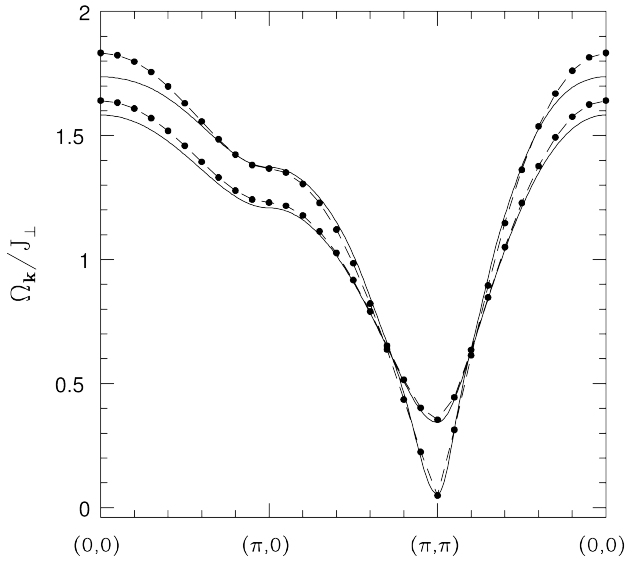

Figure 2.4: ("Novel Approach to Description of Spin Liquid Phases in Low Dimensional Quamtum Antiferromagnets", V. Kotov *et al.*, PRL, vol. **80** 26) Plot of triplet excitation spectrum for high symmetry momenta for coupling around the QCP. The uppercurve at $\mathbf{q} = 0$ corresponds to the coupling ratio $\frac{J_\perp}{J_\parallel} = 2.54$ and lower curves are for $\frac{J_\perp}{J_\parallel} = 3.33$. Once again the different curves correspond to different computational methods and approximations however for this thesis we have to note the distinct minimum for $\mathbf{q} = (\pi, \pi)$.

Chapter 3

Triplon Bound States

3.1 Frustrated model

In this section we introduce a frustrated term to our Heisenberg Hamiltonian (2.5),

$$H_F = J_F \sum_{\langle i,j \rangle} \left(\mathbf{S}_{1,i} \cdot \mathbf{S}_{2,j} + \mathbf{S}_{2,i} \cdot \mathbf{S}_{1,j} \right). \tag{3.1}$$

This term corresponds to an antiferromagnetic interaction between diagonal sites in the bilayer model. This is shown diagramatically in Figure 3.1 for a single square lattice along with intra- and inter-layer coupling. This frustrated term is important as it increases the depth of the well and provides us a new parameter to tune the depth of the bound state. This term does not change the kinematic structure of the Hamiltonian in (2.5), only the magnitudes which is beneficial in increasing the depth of the potential well as we will see in the Hamiltonian below. We define the variables,

$$J'' = J_{\parallel} + J_F,$$
$$J' = J_{\parallel} - J_F.$$

Which act as our coupling parameters we will use to vary the bound state strength.

Using the process in Appendix B the new bond operator form of the bilayer Hamilto-

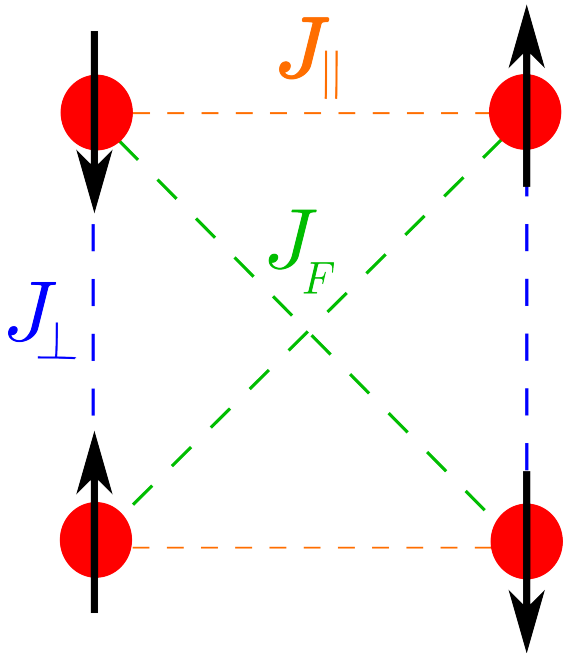

Figure 3.1: AFM coupling in the cross-section of a frustrated bilayer model (All couplings are positive).

nian is,

$$
\begin{aligned}
H_{eff} &= H_2 + H_3 + H_4, \qquad (3.2)\\
\text{Where } H_2 &= \sum_{\mathbf{k},\alpha} \left\{ A'_{\mathbf{k}} t^\dagger_{\mathbf{k}\alpha} t_{\mathbf{k}\alpha} + \frac{B'_{\mathbf{k}}}{2} \left(t^\dagger_{\mathbf{k},\alpha} t^\dagger_{\mathbf{k}\alpha} + t_{\mathbf{k}\alpha} t_{\mathbf{k}\alpha} \right) \right\},\\
H_3 &= 0,\\
H_4 &= \frac{J''}{2} \sum_{\langle i,j \rangle} \left[t^\dagger_{\alpha i} t^\dagger_{\beta j} t_{\beta i} t_{\alpha j} - t^\dagger_{\alpha i} t^\dagger_{\alpha j} t_{\beta i} t_{\beta j} \right].
\end{aligned}
$$

Where,

$$
\begin{aligned}
A'_{\mathbf{k}} &= J_\perp + 2J',\\
B'_{\mathbf{k}} &= 2J' \xi_{\mathbf{k}}.
\end{aligned}
$$

Along with the same hardcore restraint. Therefore using the same process in section 2.4 we find that addition of the frustrated term shifts the band-gap to,

$$
\begin{aligned}
\omega'^2_{\mathbf{k}} &= \sqrt{J_\perp^2 + 4J' J_\perp \xi_{\mathbf{k}}}, \qquad (3.3)\\
\Rightarrow \omega'_{\mathbf{k}} &\approx J_\perp + 2J' \xi_{\mathbf{k}}.
\end{aligned}
$$

In the highly disorder regime ($J_\perp \gg J'$). This frustrated model is also commonly studied in the literature and is thought to have many natural analogs[47, 48].

3.2 Bethe-Salpeter Equation

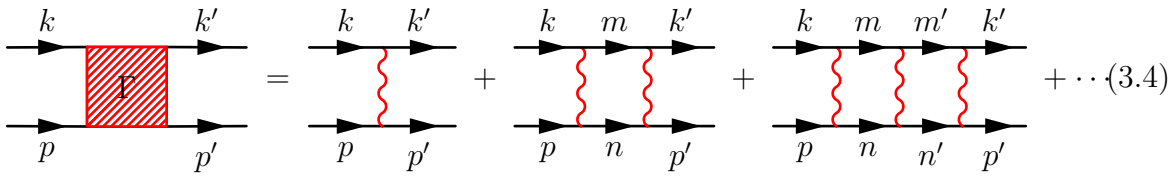

(3.4)

The Bethe-Salpeter equation [49, 50] equation is used to find the bound state between two particles. For the interaction between two states, this scattering can be represented as the infinite perturbation in (3.4).

Mathematically this is given by,

$$\Gamma_{\mathbf{kp},\mathbf{k'p'}}(E) = M_{\mathbf{kp},\mathbf{k'p'}} + \sum_{\mathbf{nm}} \frac{M_{\mathbf{kp},\mathbf{nm}} M_{\mathbf{nm},\mathbf{k'p'}}}{E - \epsilon_{\mathbf{mn}} + i0} + \sum_{\mathbf{nmn'm'}} \frac{M_{\mathbf{kp},\mathbf{nm}} M_{\mathbf{nm},\mathbf{n'm'}} M_{\mathbf{n'm'},\mathbf{k'p'}}}{E - \epsilon_{\mathbf{nm}} - \epsilon_{\mathbf{n'm'}} + i0} + \dots$$

Where $M_{i,j}$ is the Born amplitude for the scattering between states i and j and ϵ_i is the energy of the intermediate state. Upon inspection of Figure 3.4 we can see that this scattering amplitude is a geometric product. This is shown diagrammatically in (3.5).

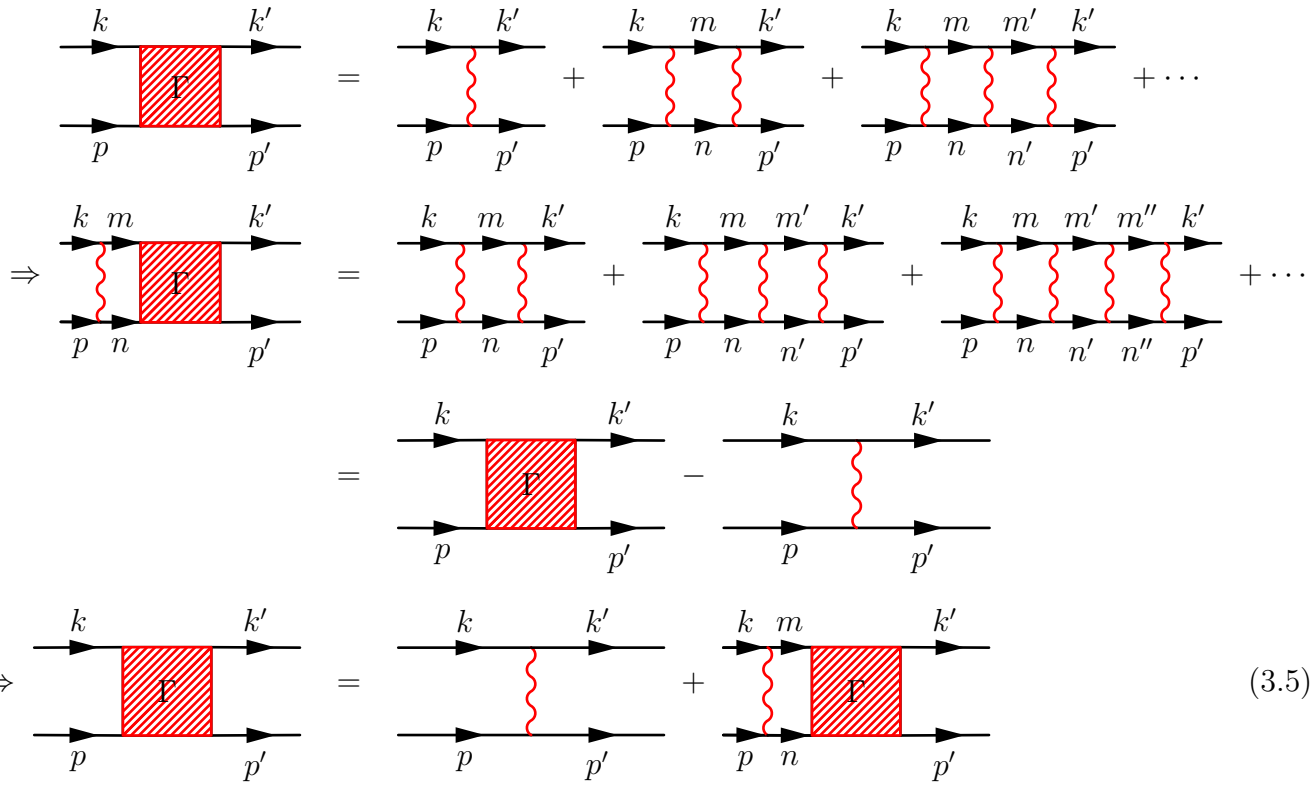

(3.5)

This is the diagram form of the Bethe-Salpeter equation, it is equivalent to the mathematical form,

$$\Gamma_{\mathbf{kp},\mathbf{k'p'}}(E) = M_{\mathbf{kp},\mathbf{k'p'}} + \sum_{\mathbf{nm}} \frac{M_{\mathbf{kp},\mathbf{nm}}\Gamma_{\mathbf{nm},\mathbf{k'p'}}(E)}{E - \epsilon_{\mathbf{n}} - \epsilon_{\mathbf{m}} + i0} \tag{3.6}$$

Where the $i0$ term corresponds to shifting the pole of the Green's function, however we will ignore this term in future calculations as it does not play a role in our model.

Therefore the Bethe-Salpeter equation changes the infinite sum of the scattering amplitude into a closed form equation. One more important step still remains, in a bound state there is a pole in the scattering amplitude and therefore approaches infinity[50]. That is,

$$E = E_B \Rightarrow \Gamma(E) \to \infty.$$

Therefore from (3.6) we can see that both the terms containing the scattering amplitude approach infinity however the first order Born approximation term remains constant

and can be ignored. Therefore for the bound state we find that,

$$\Gamma_{\mathbf{kp},\mathbf{k'p'}}(E) = \sum_{\mathbf{nm}} \frac{M_{\mathbf{kp},\mathbf{nm}}\Gamma_{\mathbf{nm},\mathbf{k'p'}}(E)}{E - \epsilon_{\mathbf{n}} - \epsilon_{\mathbf{m}} + i0}. \tag{3.7}$$

3.3 Bethe-Salpeter Equation for Triplon Bound State

For the bound state of two triplons we will use a similar approach to that of O.P. Sushkov and V.N. Kotov in [51]. The difference between these two problems is that in [51] they find the bound state in for a single 2D antiferromagnetic spin chain where we consider the 2D Bilayer. For two triplons in our bilayer with momentum $\mathbf{k}$ and $\mathbf{l}$ with a bound state energy E, the Bethe-Salpeter equation (3.7) becomes,

$$\sum_{\mathbf{k'l'}} \Gamma_{\mathbf{kk'},\mathbf{ll'}}(E) = \sum_{\mathbf{k'},\mathbf{l'}} \frac{\sum_{\mathbf{mn}} M_{\mathbf{nk'},\mathbf{ml'}}\Gamma_{\mathbf{mk'},\mathbf{nl'}}(E)}{E - \epsilon_{\mathbf{m}} - \epsilon_{\mathbf{n}}},$$

and diagramatically as (suppressing spin),

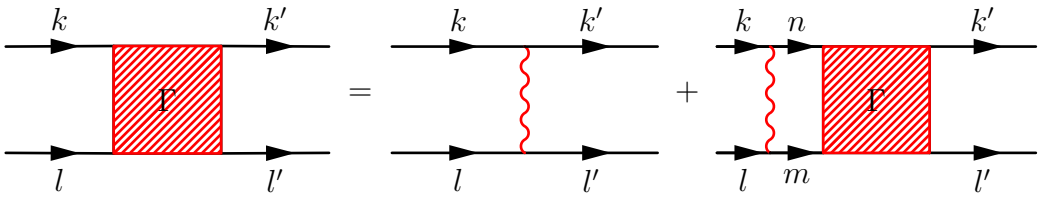

(3.8)

Letting $F_{a,b} = \sum_{a',b'} \Gamma_{aa',bb'}$ we can rearrange this into,

$$F_{\mathbf{k},\mathbf{l}}(E) = \sum_{\mathbf{mn}} \frac{M_{\mathbf{kn},\mathbf{lm}}F_{\mathbf{m},\mathbf{n}}(E)}{E - \varepsilon_{\mathbf{m}} - \varepsilon_{\mathbf{n}}},$$

and then for,

$$\psi(a,b) = \frac{F_{a,b}}{E - \epsilon_a - \epsilon_b},$$

and integrating over all possible intermediate states $\mathbf{m}$ and $\mathbf{n}$ we have the integral form of the equation,

$$(E - \epsilon_{\mathbf{k}} - \epsilon_{\mathbf{l}})\,\psi(\mathbf{k},\mathbf{l}) = \iint M_{\mathbf{km},\mathbf{ln}}\psi(\mathbf{m},\ \mathbf{n})\,d\mathbf{m}d\mathbf{n}. \tag{3.9}$$

This equation is for the two particle representation in (3.8). However as our interaction is non retarding we can reduce this two body problem to an effective one body problem by considering the centre of mass (CoM). Therefore, for the two particle scattering

$\mathbf{k}+\mathbf{l}=\mathbf{k}'+\mathbf{l}'$ we can redefine this for the total momentum of the pair,$\mathbf{Q}$ (also within the Brillouin zone), and the relative momentum ($\mathbf{q}$ and $\mathbf{p}$),

$$\begin{aligned}\text{Total Momentum: } \mathbf{Q}&=\mathbf{k}+\mathbf{l}=\mathbf{k}'+\mathbf{l}', \\ \text{Relative Momentum: } \mathbf{q}&=\frac{\mathbf{l}-\mathbf{q}}{2} \text{ and } \mathbf{p}=\frac{\mathbf{l}'-\mathbf{q}'}{2}. \\ \Rightarrow \mathbf{k}&=\frac{\mathbf{Q}}{2}+\mathbf{q}, \\ \mathbf{l}&=\frac{\mathbf{Q}}{2}-\mathbf{q}, \\ \mathbf{k}'&=\frac{\mathbf{Q}}{2}+\mathbf{p}, \\ \mathbf{l}'&=\frac{\mathbf{Q}}{2}-\mathbf{p}\end{aligned} \tag{3.10}$$

After making this transformation to relative momenta we need to be wary of double counting within the Brillouin zone for our intermediate states in (3.9). To see this consider the Brillouin zone in Figure 3.2. We see that by integrating states with positive momentum in the x direction within the Brillouin zone by symmetry we also integrate over negative momenta. Therefore to avoid this double counting we have divide the sum over the Brillouin zone by 2.

Obviously the intermediate energies of the triplons must obey the triplon dispersion relation (3.3) that is,

$$\begin{aligned}\epsilon_i&=\omega_i' \\ \Rightarrow \epsilon_{\mathbf{k}}+\epsilon_{\mathbf{l}}&=\omega'_{\frac{\mathbf{Q}}{2}-\mathbf{q}}+\omega'_{\frac{\mathbf{Q}}{2}+\mathbf{q}},\end{aligned}$$

After applying these conditions, we find that the BSE in its discrete sum form is given by,

$$\left(E-\omega'_{\frac{\mathbf{Q}}{2}+\mathbf{q}}-\omega'_{\frac{\mathbf{Q}}{2}+\mathbf{q}}\right)\psi\left(\mathbf{Q},\mathbf{q}\right)=\frac{1}{2}\sum_{\mathbf{q}}M\left(\mathbf{Q},\mathbf{q},\mathbf{p}\right)\psi\left(\mathbf{p}\right) \tag{3.11}$$

3.3.1 Born Approximation

To solve (3.11) we need to calculate the scattering amplitude of the Born approximation for the initial state into the intermediate states,

$$M_{\alpha\beta,\gamma\delta}\left(\mathbf{Q},\mathbf{q},\mathbf{p}\right). \tag{3.12}$$

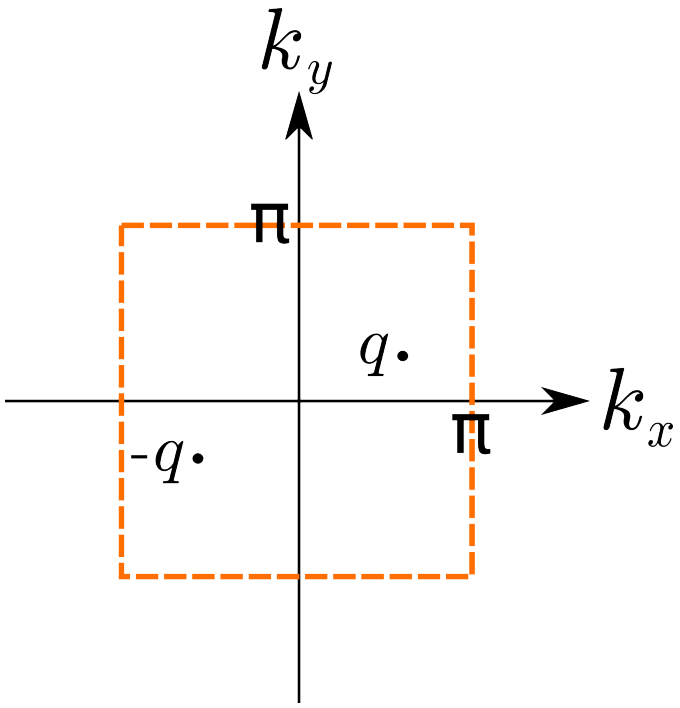

Figure 3.2: Brillouin zone for our simple square lattice. For some $\mathbf{q}$ in the region $q_x > 0$ we also have the opposite momenta $-\mathbf{q}$. Therefore to avoid this double counting we divide the sum by 2.

Therefore we will first consider how the Born scattering changes the momentum of the system.

As we are considering a two dimensional square lattice we can split up the scattering

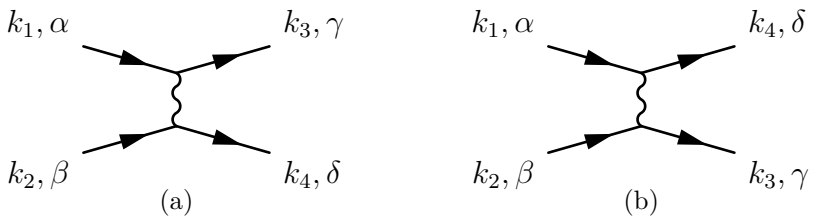

Figure 3.3: The two Born scattering processes for arbitrary initial, $\mathbf{k}_1$ and $\mathbf{k}_2$, and final momenta, $\mathbf{k}_3$ and $\mathbf{k}_4$, with spin polarisations $\alpha, \beta, \gamma, \delta$.

problem into two dimensions, x and y (Figure 3.4) and consider them separately. First we need to transform our quartic hamiltonian (**??**) into momentum space. To do this we use the standard Fourier transform with respect to the discrete lattice sites i and j using equation (2.6), where here, to avoid confusion, we reference the lattice points as

r_i, assume a summation over all equations and ignore the normalisation of the finite lattice, N.

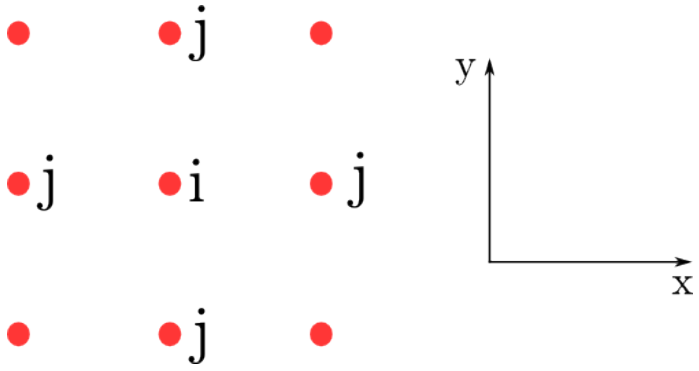

Figure 3.4: The square lattice of our bilayer. This allows us to separate the system into x and y components.

To find the Born scattering amplitude we have to find the matrix elements of the the quartic Hamiltonian (3.2) with the initial and final states in Figure 3.3a,

$$H_4 = \frac{J''}{2} \sum_{k,\langle r_i, r_j \rangle} e^{i(k_1 r_i + k_2 r_j - k_3 r_i - k_4 r_j)} \left[t^\dagger_{\alpha,k_3} t^\dagger_{\beta,k_4} t_{\beta,k_1} t_{\alpha,k_2} - t^\dagger_{\alpha,k_3} t^\dagger_{\alpha,k_4} t_{\beta,k_1} t_{\beta,k_2} \right].$$

Now summing over nearest neighbours (Figure 3.4) we have that,

$$\begin{aligned} r_j &= r_i \pm 1, \\ \Rightarrow \sum_{\langle r_i, r_j \rangle} &= \sum_{r_i} \left\{ (r_j \to r_i + 1) + (r_j \to r_i - 1) \right\}. \end{aligned}$$

Therefore,

$$\begin{aligned} \sum_{r_i, r_i+1} H_4 + \sum_{r_i, r_i-1} H_4 = \frac{J''}{2} & e^{i(k_1 r_i + k_2 r_i - k_3 r_i - k_4 r_i)} \left(e^{i(k_2 - k_4)} + e^{-i(k_2 - k_4)} \right) \times \\ & \left[t^\dagger_{\alpha,k_3} t^\dagger_{\beta,k_4} t_{\beta,k_1} t_{\alpha,k_2} - t^\dagger_{\alpha,k_3} t^\dagger_{\alpha,k_4} t_{\beta,k_1} t_{\beta,k_2} \right], \\ = J'' & e^{i(k_1 r_i + k_2 r_i - k_3 r_i - k_4 r_i)} \cos(k_2 - k_4) \left[t^\dagger_{\alpha,k_3} t^\dagger_{\beta,k_4} t_{\beta,k_1} t_{\alpha,k_2} - t^\dagger_{\alpha,k_3} t^\dagger_{\alpha,k_4} t_{\beta,k_1} t_{\beta,k_2} \right]. \end{aligned}$$

Therefore the scattering amplitude is given by,

$$\begin{aligned} M_{\alpha\beta,\gamma\delta}(k) &= \frac{J''}{2}\left\langle t_{\delta,k_4}t_{\gamma,k_3}\left|H_4\right|t^\dagger_{\alpha,k_1}t^\dagger_{\beta,k_2}\right\rangle \\ &= J''e^{i(k_1r_i+k_2r_i-k_3r_i-k_4r_i)}\cos(k_2-k_4)\times \\ &\left\langle t_{\delta,k_4}t_{\gamma,k_3}\left|t^\dagger_{\alpha,k_3}t^\dagger_{\beta,k_4}t_{\beta,k_1}t_{\alpha,k_2}-t^\dagger_{\alpha,k_3}t^\dagger_{\alpha,k_4}t_{\beta,k_1}t_{\beta,k_2}\right|t^\dagger_{\alpha,k_1}t^\dagger_{\beta,k_2}\right\rangle, \\ &= J''e^{i(k_1r_i+k_2r_i-k_3r_i-k_4r_i)}\cos(k_2-k_4)\left(\delta_{\alpha\delta}\delta_{\beta\gamma}-\delta_{\alpha\beta}\delta_{\gamma\delta}\right). \end{aligned}$$

This is for the scattering in Figure 3.3a, in Born scattering there are two possible scattering due to the indistinguisability of the particle, therefore for the second scattering event (Figure 3.3b) we simply have $k_4 \leftrightarrow k_3$. which implies the other scattering event is,

$$\begin{aligned} M_{\alpha\beta,\gamma\delta}(k) &= J''e^{i(k_1r_i+k_2r_i-k_3r_i-k_4r_i)}\cos(k_2-k_3)\times \\ &\left\langle t_{\delta,k_4}t_{\gamma,k_3}\left|t^\dagger_{\alpha,k_3}t^\dagger_{\beta,k_4}t_{\alpha,k_1}t_{\beta,k_2}-t^\dagger_{\alpha,k_3}t^\dagger_{\alpha,k_4}t_{\beta,k_1}t_{\beta,k_2}\right|t^\dagger_{\alpha,k_1}t^\dagger_{\beta,k_2}\right\rangle, \\ &= 2e^{i(k_1r_i+k_2r_i-k_3r_i-k_4r_i)}\cos(k_2-k_3)\left(\delta_{\alpha\gamma}\delta_{\beta\delta}-\delta_{\alpha\beta}\delta_{\gamma\delta}\right). \end{aligned}$$

Now substituting in the CoM momenta in the x-direction,

$$\begin{aligned} k_1 &= \frac{Q_x}{2}+q_x, \\ k_2 &= \frac{Q_x}{2}-q_x, \\ k_3 &= \frac{Q_x}{2}+q'_x, \\ k_4 &= \frac{Q_x}{2}-q'_x. \end{aligned}$$

The total Born approximation for the x-direction becomes,

$$M_{\alpha\beta,\gamma\delta}(\mathbf{q})_x = J''\left(\delta_{\alpha\gamma}\delta_{\beta\delta}-\delta_{\alpha\beta}\delta_{\gamma\delta}\right)\cos(q_x+q'_x)+J''\left(\delta_{\alpha\delta}\delta_{\beta\gamma}-\delta_{\alpha\beta}\delta_{\gamma\delta}\right)\cos(q_x-q'_x).$$

The Born amplitude is the same for the y-direction. Therefore in total the Born Amplitude is,

$$\begin{aligned} M_{\alpha\beta,\gamma\delta}(k) &= 2J''\left(\delta_{\alpha\gamma}\delta_{\beta\delta}-\delta_{\alpha\beta}\delta_{\gamma\delta}\right)\xi_{q+q'}+2J''\left(\delta_{\alpha\delta}\delta_{\beta\gamma}-\delta_{\alpha\beta}\delta_{\gamma\delta}\right)\xi_{q-q'}, \\ \text{For } \xi_k &= \frac{1}{2}\left(\cos(k_x)+\cos(k_y)\right). \end{aligned} \tag{3.13}$$

To define a definitive Born amplitude we need to define our spin polarisations. In

the case of the bound state between two triplons there are 3 possible spin channels. The first is the unpolarised state where the the total spin of the bound state is $S = 0$, the second is the triplet channel where the total spins add up to $S = 1$ and finally is the state is the quadrapole channel where the total spins add up to $S = 2$. These channels are discussed in depth in Appendix C and in this thesis we will consider the bound states for all three channels.

3.3.2 Dispersion Relation

For our system the energy of the incident particles is given by the quasi-particle excitation spectrum, and as we are considering the highly disordered phase ($J_\perp \gg J_\parallel$) we use (2.10). Therefore substituting in the CoM momentum terms we have that,

$$\begin{aligned}
\varepsilon_{\mathbf{k}} &= \omega'_{\frac{\mathbf{Q}}{2}+\mathbf{q}}, \\
\varepsilon_{\mathbf{p}} &= \omega'_{\frac{\mathbf{Q}}{2}-\mathbf{q}} \\
\omega_{\frac{\mathbf{Q}}{2}+\mathbf{q}} + \omega_{\frac{\mathbf{Q}}{2}-\mathbf{q}} &= 2J_\perp + 2J' \left[\xi_{\frac{\mathbf{Q}}{2}+\mathbf{q}} + \xi_{\frac{\mathbf{Q}}{2}+\mathbf{q}}\right], \\
&= 2J_\perp + J' \left[\cos\left(\frac{Q_x}{2} + q_x\right) + \cos\left(\frac{Q_y}{2} + q_y\right) + \cos\left(\frac{Q_x}{2} - q_x\right) + \cos\left(\frac{Q_y}{2} - q_y\right)\right], \\
&= 2J\perp + 2J' \left[\cos\left(\frac{Q_x}{2}\right)\cos\left(q_x\right) + \cos\left(\frac{Q_y}{2}\right)\cos\left(q_y\right)\right].
\end{aligned}$$

With this equation the energy spectrum is given by,

$$\left[E - \omega'_{\frac{\mathbf{Q}}{2}+\mathbf{q}} + \omega'_{\frac{\mathbf{Q}}{2}-\mathbf{q}}\right] = \left\{E + 2J_\perp + 2J' \left[\cos\left(\frac{Q_x}{2}\right)\cos\left(q_x\right) + \cos\left(\frac{Q_y}{2}\right)\cos\left(q_y\right)\right]\right\}.$$

Similar to [51] we define a positive bound state energy (ε_B) to be the energy of the scattered states below the minimum of the dispersion, that is,

$$\varepsilon_B = E^c_{\mathbf{q}} - E > 0.$$

As mentioned in the previous chapter the minimum of of the dispersion relation occurs at, $(q_x, q_y) = (\pi, \pi)$ (Figure 2.4) and therefore the minimum is given by,

$$E^c_{\mathbf{q}} = 2J_\perp - 2J' \left[\cos\left(\frac{Q_x}{2}\right) + \cos\left(\frac{Q_y}{2}\right)\right],$$

and therefore we can rewrite the above equation as,

$$-\varepsilon_B - 2J' \left[\cos\left(\frac{Q_x}{2}\right)(1+\cos(q_x)) + \cos\left(\frac{Q_y}{2}\right)(1+\cos(q_y)) \right].$$

Therefore extracting the coupling constant leaves us with,

$$-J' \left\{ \frac{\varepsilon_B}{J'} + 2 \left[\cos\left(\frac{Q_x}{2}\right)(1+\cos(q_x)) + \cos\left(\frac{Q_y}{2}\right)(1+\cos(q_y)) \right] \right\} \tag{3.14}$$

3.4 Wavefunction of Triplon Bound State

We can define the wavefunction of the bound state of two triplons with momentum $\mathbf{l}$ and $\mathbf{k}$ and polarisation α and β in momentum space as,

$$\Psi(\mathbf{k},\mathbf{l})\, \tau^\dagger_{\mathbf{kl},\alpha\beta} |0\rangle = \sum_{\mathbf{k},\mathbf{l}} \psi(\mathbf{k},\mathbf{l})\, t^\dagger_{\mathbf{k},\alpha} t^\dagger_{\mathbf{l},\beta} |0\rangle$$

and therefore converting it into a relative frame and using (3.10) we have,

$$\Psi(\mathbf{q},\mathbf{Q})\, \tau^\dagger_{\mathbf{Q},\alpha\beta} |0\rangle = \sum_{\mathbf{q}>0} \psi(\mathbf{q},\mathbf{Q})\, t^\dagger_{\frac{\mathbf{Q}}{2}+\mathbf{q},\alpha} t^\dagger_{\frac{\mathbf{Q}}{2}-\mathbf{q},\beta} |0\rangle .$$

Where again we only consider the sum over the right half of the Brillouin zone to avoid double counting ($\mathbf{q} > 0$). Therefore we now apply the normalisation condition, however we need to be careful about summing up all possible polarisation of the triplon states. To see this we have to individually consider the spin channels which are covered in appendix C. We denote the square of the normalisation coefficient for each separate channel as P^2. Therefore the normalisation condition becomes.

$$\begin{aligned} |\Psi(\mathbf{q},\mathbf{Q})|^2 \left\langle 0 \left| \tau_{\mathbf{Q},\alpha\beta} \tau^\dagger_{\mathbf{Q},\alpha\beta} \right| 0 \right\rangle &= 1, \\ \Rightarrow P^2 \sum_{\mathbf{q}>0} |\psi(\mathbf{q},\mathbf{Q})|^2 \left\langle 0 \left| t_{\frac{\mathbf{Q}}{2}+\mathbf{q},\alpha} t_{\frac{\mathbf{Q}}{2}-\mathbf{q},\beta} t^\dagger_{\frac{\mathbf{Q}}{2}+\mathbf{q},\alpha} t^\dagger_{\frac{\mathbf{Q}}{2}-\mathbf{q},\beta} \right| 0 \right\rangle &= 1, \\ \Rightarrow P^2 \sum_{\mathbf{q}>0} |\psi(\mathbf{q},\mathbf{Q})|^2 &= 1. \end{aligned}$$

Therefore shifting the sum to the entire Brillouin zone and transforming into integral form we have the normalisation condition,

$$\frac{P^2}{2}\sum_{\mathbf{q}}\left|\psi\left(\mathbf{q},\mathbf{Q}\right)\right|^2 = 1,$$
$$\Rightarrow \frac{P^2}{2}\iint_{-\pi}^{\pi}\left|\psi\left(\mathbf{q},\mathbf{Q}\right)\right|^2\frac{1}{\left(2\pi\right)^2}d^2\mathbf{q} = 1.. \tag{3.15}$$

In the context of bound states an interesting property of the wavefunction is the Root-Mean Square (RMS) of its diameter, ($D^2_{RMS} = \langle d^2\rangle$) [51]. The RMS diameter of the wavefunction will represent the spatial extent of the bound state on the bilayer. To find the RMS diameter of the bound state we first consider the expectation value of the diameter squared on the bilayer,

$$\langle d^2\rangle = P^2\iint_{-\infty}^{\infty}\psi^*\left(\mathbf{r}\right)\hat{d}^2\psi\left(\mathbf{r}\right)d^2\mathbf{r}.$$

Transferring this into momentum space leaves us with,

$$\begin{aligned}\langle d^2\rangle &= -P^2\iint_{-\infty}^{\infty}\left(-i\frac{\partial}{\partial\mathbf{q}}\psi\left(\mathbf{q}\right)\right)^*\left(i\frac{\partial}{\partial\mathbf{q}}\psi\left(\mathbf{q}\right)\right)d^2\mathbf{q},\\ &= P^2\iint_{-\infty}^{\infty}\left|\frac{\partial\psi\left(\mathbf{q}\right)}{\partial\mathbf{q}}\right|^2 d^2\mathbf{q}.\end{aligned}$$

Therefore transforming this back into our Brillouin zone we have that the RMS diameter of the wavefunction, D_{RMS}, is given by,

$$D_{RMS} = \sqrt{\langle d^2\rangle}, \tag{3.16}$$
$$\text{Where } \langle d^2\rangle = \frac{P^2}{2}\sum_{\mathbf{q}}\left|\frac{\partial\psi\left(\mathbf{q},\right)}{\partial\mathbf{q}}\right|^2 d^2\mathbf{q}. \tag{3.17}$$

3.5 Singlet Channel Bound State, S = 0

From here on we will refer to this as the singlet bound state. Now we have the required equations for the incident energy spectrum (3.14), Born scattering dependence (3.13) and the bound state wavefunction (3.16) we can now consider certain cases for the bound states. These cases depend of the spin channels Appendix C.2. First we consider

the singlet case, in terms of the Born amplitude, the singlet channel is given by,

$$M^{(0)}(\mathbf{q}, \mathrm{p}) = \frac{1}{3}\delta_{\alpha\beta}\delta_{\gamma\delta}M_{\alpha\beta,\gamma\delta}(\mathbf{q}, \mathbf{p})$$

Expanding out the Born amplitude (3.13) we see that,

$$\begin{aligned} M^{(0)}(\mathbf{q}, \mathbf{p}) = \frac{1}{3}\delta_{\alpha\beta}\delta_{\gamma\delta}J''\left[\delta_{\alpha\gamma}\delta_{\beta\delta} + \delta_{\alpha\delta}\delta_{\beta\gamma} - 2\delta_{\alpha\beta}\delta_{\gamma\delta}\right](\cos(q_x)\cos(p_x) + \cos(q_y)\cos(p_y)) \\ -\frac{1}{3}\delta_{\alpha\beta}\delta_{\gamma\delta}J''\left[\delta_{\alpha\gamma}\delta_{\beta\delta} - \delta_{\alpha\delta}\delta_{\beta\gamma}\right](\sin(q_x)\sin(p_x) + \sin(q_y)\sin(p_y)) \\ +\frac{1}{3}\delta_{\alpha\beta}\delta_{\gamma\delta}U\left[\delta_{\alpha\gamma}\delta_{\beta\delta} + \delta_{\alpha\delta}\delta_{\beta\gamma}\right] \end{aligned} \tag{3.18}$$

Therefore using the relations,

$$\begin{aligned} \delta_{\alpha\beta}\delta_{\gamma\delta}\delta_{\alpha\beta}\delta_{\gamma\delta} &= 9, \\ \delta_{\alpha\beta}\delta_{\gamma\delta}\delta_{\alpha\gamma}\delta_{\beta\delta} &= 3, \\ \delta_{\alpha\beta}\delta_{\gamma\delta}\delta_{\alpha\delta}\delta_{\beta\gamma} &= 3. \end{aligned}$$

We see that the second term of (3.18) cancels and we are left with,

$$\begin{aligned} M^{(0)}(\mathbf{q}, \mathbf{p}) &= \frac{J''}{3}(6 - 18)(\cos(q_x)\cos(p_x) + \cos(q_y)\cos(p_y)) + \frac{6U}{3} \\ &= -4J''(\cos(q_x)\cos(p_x) + \cos(q_y)\cos(p_y)) + 2U \end{aligned}$$

Therefore the BSE for the singlet channel is,

$$\begin{aligned} \left(E - \omega'_{\frac{\mathbf{Q}}{2}+\mathbf{q}} - \omega'_{\frac{\mathbf{Q}}{2}+\mathbf{q}}\right)\psi(\mathbf{q}) = \sum_{\mathbf{p}} M^{(0)}(\mathbf{q}, \mathbf{p})\,\psi(\mathbf{p}) \\ -J'\left\{\frac{\varepsilon_B^{(0)}}{J'} + 2\left[\cos\left(\frac{Q_x}{2}\right)(1 + \cos(q_x)) + \cos\left(\frac{Q_y}{2}(1 + \cos(q_y))\right)\right]\right\}\psi(\mathbf{q}) = \\ \sum_{\mathbf{p}}\left\{-2J''\left[\cos(q_x)\cos(p_x) + \cos(q_y)\cos(p_y)\right] + 2U\right\}\psi(\mathbf{p}). \end{aligned} \tag{3.19}$$

For the singlet case we can take advantage of the C4 point group symmetry of the square lattice [52]. It is obvious that the under a 90° rotation the system is invariant. That is the wavefunction has the property,

$$\psi(q_x, q_y) = \psi(q_y, q_x). \tag{3.20}$$

Therefore in (3.19) we can reduce the RHS to,

$$-4J''\left[\cos\left(q_x\right)\sum_{p_x}\cos\left(p_x\right)\psi\left(p_x,p_y\right)+\cos\left(q_y\right)\sum_{p_y}\cos\left(p_y\right)\psi\left(p_x,p_y\right)\right]+2U\psi\left(p_x,p_y\right).$$

Therefore applying (3.20) we can see that

$$\sum_{\mathbf{p}}\cos\left(p_x\right)\psi\left(p_x,p_y\right)\equiv\sum_{\mathbf{p}}\cos\left(p_y\right)\psi\left(p_y,p_x\right).$$

Now by inspection, we can write,

$$\cos\left(q_x\right)\cos\left(p_x\right)+\cos\left(q_y\right)\cos\left(p_y\right)\rightarrow 2\xi_{\mathbf{q}}\xi_{\mathbf{p}}. \tag{3.21}$$

Therefore in the singlet channel the BSE equation is,

$$-J'\left\{\frac{\varepsilon_B}{J'}+2\left[\cos\left(\frac{Q_x}{2}\right)\left(1+\cos\left(q_x\right)\right)+\cos\left(\frac{Q_y}{2}\left(1+\cos\left(q_y\right)\right)\right)\right]\right\}\psi\left(\mathbf{q}\right)=\sum_{\mathbf{p}}\left\{-4J''\xi_{\mathbf{q}}\xi_{\mathbf{p}}+2U\right\}\psi\left(\mathbf{p}\right). \tag{3.22}$$

3.5.1 Zero Total Momentum, Q = 0

To begin the bound state calculations we consider the simplest case where the total momentum of the triplons is zero. From (3.22) the equation for our bound state is given by,

$$-J'\left[\frac{\varepsilon_B}{J'}+4+4\xi_{\mathbf{q}}\right]\psi\left(\mathbf{q}\right)=\sum_{\mathbf{p}}\left\{-4J''\xi_{\mathbf{q}}\xi_{\mathbf{p}}+2U\right\}\psi\left(\mathbf{p}\right) \tag{3.23}$$

$$\Rightarrow\psi\left(\mathbf{q}\right)=\frac{4J''}{J'}\frac{\xi_{\mathbf{q}}}{\left[\frac{\varepsilon_B}{J'}+4+4\xi_{\mathbf{q}}\right]}\sum_{\mathbf{p}}\xi_{\mathbf{p}}\psi\left(\mathbf{p}\right)-\frac{2U}{J'}\frac{1}{\left[\frac{\varepsilon_B}{J'}+4+4\xi_{\mathbf{q}}\right]}\sum_{\mathbf{p}}\psi\left(\mathbf{p}\right).$$

and therefore by inspection our wavefunction must have the form,

$$\psi\left(\mathbf{q}\right)=A\frac{C+\xi_{\mathbf{q}}}{\left[\frac{\varepsilon_B}{J'}+4+4\xi_{\mathbf{q}}\right]}. \tag{3.24}$$

Where A is some normalisation constant and C is a constant. In order to satisfy the hard core constraint of our system ($U \to \infty$) we must enforce the condition,

$$\sum_{\mathbf{q}} \psi(\mathbf{q}) = 0,$$
$$\Rightarrow \sum_{\mathbf{q}} \frac{C + \xi_{\mathbf{q}}}{\left[\frac{\varepsilon_B}{J'} + 4 + 4\xi_{\mathbf{q}}\right]} = 0, \tag{3.25}$$

to have a finite wavefunction. Therefore using (3.25) and substituting (3.24) back into (3.23) we are left with the equation,

$$C + \xi_{\mathbf{q}} = \frac{4J''}{J'}\xi_{\mathbf{q}} \sum_{\mathbf{p}} \xi_{\mathbf{p}} \frac{C + \xi_{\mathbf{p}}}{\left[\frac{\varepsilon_B}{J'} + 4 + 4\xi_{\mathbf{p}}\right]},$$

and therefore comparing coefficients we have the relation,

$$\sum_{\mathbf{p}} \xi_{\mathbf{p}} \frac{C + \xi_{\mathbf{p}}}{\left[\frac{\varepsilon_B}{J'} + 4 + 4\xi_{\mathbf{p}}\right]} = \frac{J'}{4J''}. \tag{3.26}$$

With the conditions (3.25) and (3.26) we can find the singlet bound state. First we realise that there exists an explicit relation between the the constant C and the coupling constants J' and J''. To see this we rewrite the conditions as,

$$\sum_{\mathbf{q}} \frac{C + \xi_{\mathbf{q}}}{\mathcal{D}(\mathbf{q}, \varepsilon_B)} = 0, \tag{3.27}$$
$$\sum_{\mathbf{q}} \xi_{\mathbf{q}} \frac{C + \xi_{\mathbf{q}}}{\mathcal{D}(\mathbf{q}, \varepsilon_B)} = \frac{J'}{4J''}, \tag{3.28}$$
$$\text{Where } \mathcal{D}(\mathbf{q}, \varepsilon_B) = \left[\frac{\varepsilon_B}{J'} + 4 + 4\xi_{\mathbf{q}}\right], \tag{3.29}$$
$$\Rightarrow \xi_{\mathbf{q}} = \frac{\mathcal{D}(\mathbf{q}, \varepsilon_B)}{4} - \frac{\varepsilon_B}{4J'} - 1. \tag{3.30}$$

Substituting (3.30) into both (3.27) and (3.28) we have that,

$$\left(C - \frac{\varepsilon_B}{J'} - 1\right) \sum_{\mathbf{q}} \frac{1}{\mathcal{D}(\mathbf{q}, \varepsilon_B)} + \frac{1}{4} = 0, \tag{3.31}$$
$$\frac{C}{4} - \frac{1}{2}\left(\frac{\varepsilon_B}{J'} + 1\right) - \frac{\varepsilon_B}{J'} + 1(C - \frac{\varepsilon_B}{J'} + 1) \sum_{\mathbf{q}} \frac{1}{\mathcal{D}(\mathbf{q}, \varepsilon_B)} = \frac{J'}{4J''}. \tag{3.32}$$

Subsitituting (3.31) into (3.32) and evaluating the sum gives the relation,

$$\frac{C}{4} - \frac{1}{4}\left(\frac{\varepsilon_B}{J'} + 1\right) - \frac{\varepsilon_B}{J'} + 1(C - \frac{\varepsilon_B}{J'} + 1)\left(\frac{1}{4}\right) = \frac{J'}{4J''},$$
$$\Rightarrow C = \frac{J'}{J''}. \tag{3.33}$$

Therefore we have a simple relation between the constant and the coupling constants.

Critical Coupling

We now look for the critical coupling for the singlet bound state. The critical coupling is the smallest required coupling for a bound state to exist. Therefore we have to find $\frac{J''}{J'}$ in the limit $\varepsilon_B \to 0+$. Therefore for critical coupling (3.25) becomes,

$$\sum_{\mathbf{q}} \frac{C_{crit} + \xi_{\mathbf{q}}}{[4 + 4\xi_{\mathbf{q}}]} = 0.$$

This equation has a singluarity at $(q_x, q_y) = (\pi, \pi)$ and therefore we must also satisfy the condition,

$$C_{crit} + \xi_{\mathbf{q}} = 0 \text{ for } (q_x, q_y) = (\pi, \pi),$$
$$\Rightarrow C_{crit} = 1.$$

and therefore from (3.33),

$$\left(\frac{J''}{J'}\right)_{crit} = 1.$$

Therefore in the singlet channel for $\frac{J''}{J'} < 1$ there are no bound states for $\mathbf{Q} = 0$.

Strong Coupling

Now we look at the strong coupling limit for the bound state, that is for the coupling $J'' \gg J'$. In this coupling we effectively have a very deep well and therefore our bound state is also large($\varepsilon_B \gg J'$). By inspection we see that $C \to 0$ from (3.33) and therefore the wavefunction of the in the strong coupling regime is,

$$\psi(\mathbf{q}) = A\frac{\xi_{\mathbf{q}}}{\varepsilon_B}.$$

Using the normalisation condition (3.15) we then have that,

$$\begin{aligned}\frac{3}{2}A^2\sum_{\mathbf{q}}\frac{\xi_{\mathbf{q}}^2}{\varepsilon_B^2} &= 1,\\ \Rightarrow A &= \sqrt{\frac{8}{3}}\varepsilon_B.\end{aligned}$$

and therefore the strong coupling wavefunction is,

$$\psi\left(\mathbf{q}\right) = \sqrt{\frac{8}{3}}\xi_{\mathbf{q}}. \tag{3.34}$$

We can also write (3.26) as,

$$\begin{aligned}\sum_{\mathbf{q}}\frac{\xi_{\mathbf{q}}^2}{\frac{\varepsilon_B}{J'}} &= \frac{J'}{4J''},\\ \Rightarrow \varepsilon_B &= J''.\end{aligned} \tag{3.35}$$

Therefore for large coupling the binding energy is equal to J''.

We also have that the RMS diameter in the strong coupling regime is given by (3.16) and therefore using (3.34) we have that,

$$\begin{aligned}\langle d^2\rangle &= \frac{8}{2}\iint_{-\pi}^{\pi}\zeta_{\mathbf{q}}\frac{1}{\left(2\pi\right)^2}d^2\mathbf{q},\\ &= 1,\\ \text{Where } \zeta_{\mathbf{k}} &= \frac{1}{2}\left(\sin\left(k_x\right)+\sin\left(k_y\right)\right),\\ \Rightarrow R_{RMS} &= 1.\end{aligned} \tag{3.36}$$

Therefore in the strong coupling regime the RMS diameter of the wavefunction approaches the value of a lattice spacing (which we assume to be one, $a = 1$) as expected.

Bound State vs Coupling Constant

The equations (3.25) and (3.26) are elliptical functions and therefore cannot be solved analytically. However they can be solved numerically using the simple method outlined in appendix D. Using (3.33) we can reduce the problem down to one numerical equation

we need to solve.

$$\text{Sum} = \sum_{\mathbf{q}} \frac{\frac{J'}{J''} + \xi_{\mathbf{q}}}{\left[\frac{\varepsilon_B}{J'} + 4 + 4\xi_{\mathbf{q}}\right]} = 0. \tag{3.37}$$

To solve this equation for a particular coupling ratio $\frac{J''}{J'}$ (and similar ones for the remainder of the thesis) we can compute and plot the above sum for a reasonable spectrum of unitless energies $\frac{\varepsilon_B}{J'}$ and where the plot crosses the axis is the unitless binding energy for the particular coupling ratio which we will now refer to as the binding energy vs coupling constant. For $\frac{J''}{J'} = 3$ and in the range $\frac{\varepsilon_B}{J'} \in (0, 1)$ we plot (3.37) vs $\frac{\varepsilon_B}{J'}$ in Figure 3.5. Therefore to produce a plot of binding energy vs the coupling constant

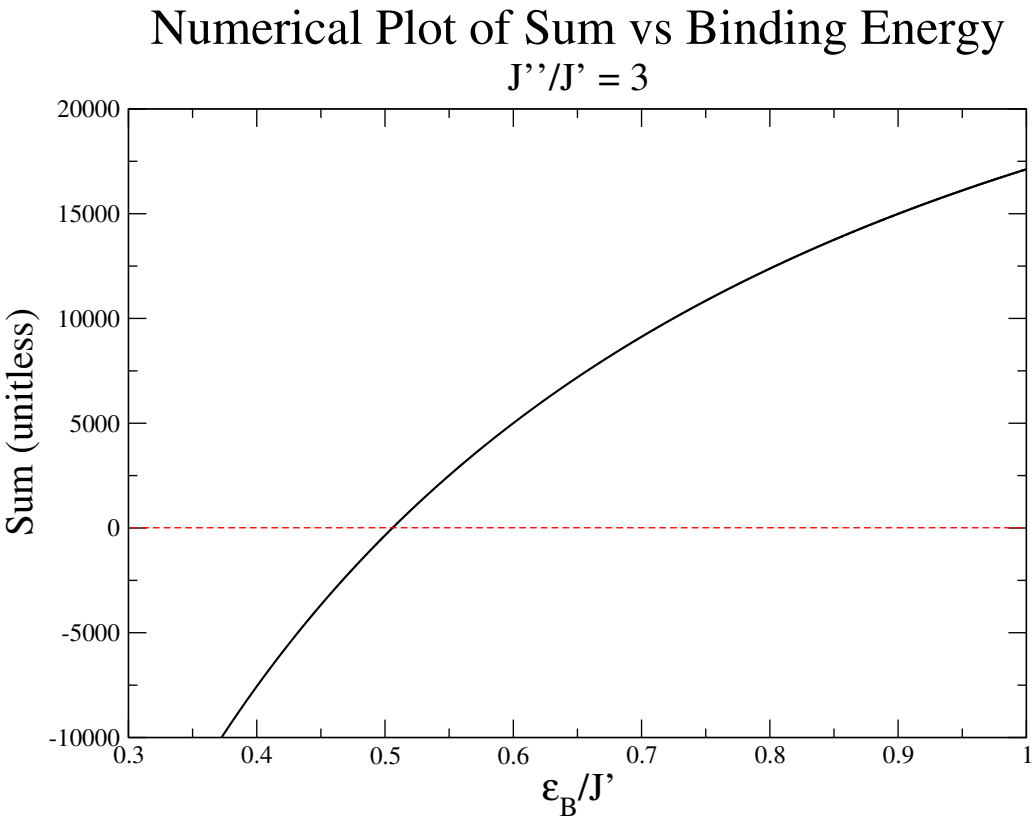

Figure 3.5: This is is numeric plot of the LHS of Sum vs $\frac{\varepsilon_B}{J'}$. There is bound state for the root of this plot which was found to numerically be $\frac{\varepsilon_B}{J'} \approx 0.50600$.

we just plot the numerical roots of the equation for each respective coupling constant. The resultant plot of this for $\frac{J''}{J'} \in (0, 7)$ and $\frac{\varepsilon_B}{J'} \in (0, 2)$ is given in Figure 3.6. As we can see from Figure 3.6 there exists no bound states for $\frac{J''}{J'} < 1$ as predicted. For $\frac{J''}{J'} \to 1+$ the numerical approach starts to fail which is why the plot produces a critical

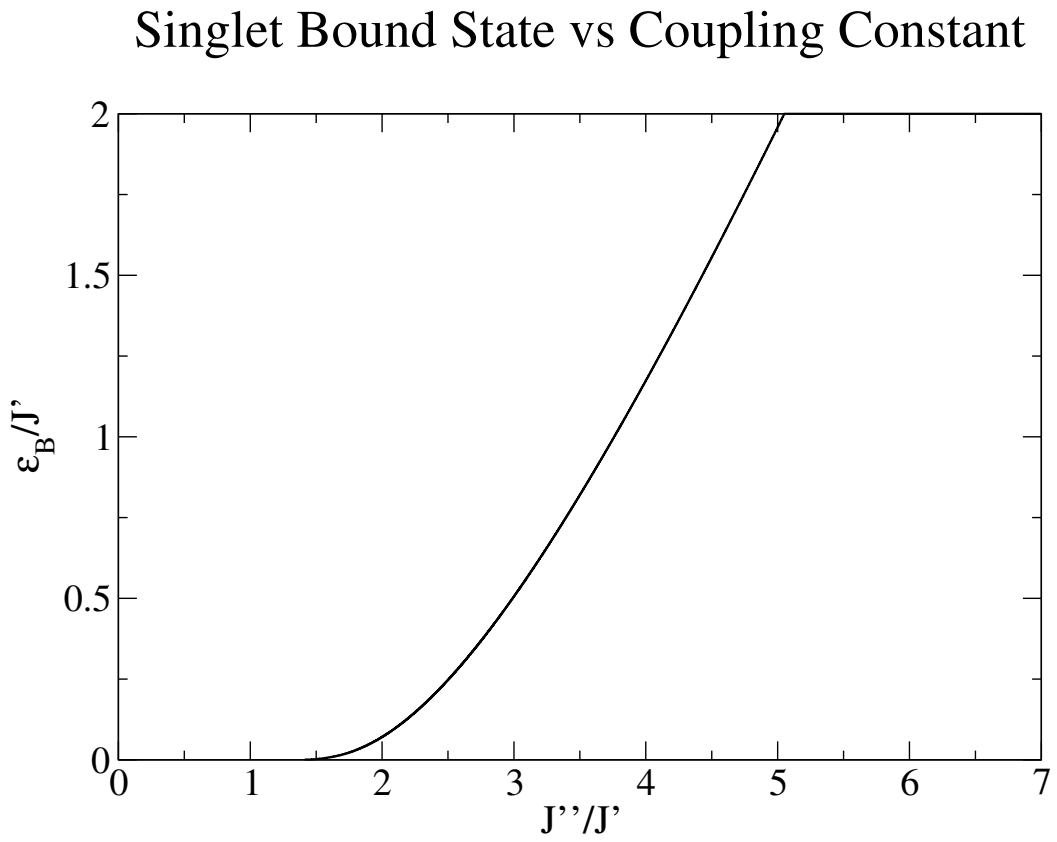

Figure 3.6: Singlet Bound State vs Coupling Constant. This is the Numeric Plot of the roots of (3.37) for each coupling constant.

coupling of $\left(\frac{J''}{J'}\right) \approx 1.5$.

We now also find the how the RMS diameter of the wavefunction depends on the coupling constant. Once again due to the non-analytic nature of the system we have to approach this analytically. Considering the singlet wavefunction (3.24), the normalisation condition (3.15) and the RMS form we have the following relations,

$$\begin{aligned}
\langle d^2 \rangle &= \frac{3}{2} A^2 \iint_{-\pi}^{\pi} \left| \frac{\partial}{\partial \mathbf{q}} \frac{\frac{J''}{J'} + \xi_{\mathbf{q}}}{\left[\frac{\varepsilon_B}{J'} + 4 + 4\xi_{\mathbf{q}}\right]} \right|^2 \frac{1}{(2\pi)^2} d^2\mathbf{q} \\
&= \frac{3\,|A|^2}{2} \iint_{-\pi}^{\pi} \left| \frac{\zeta_{\mathbf{q}}}{\left[\frac{\varepsilon_B}{J'} + 4 + 4\xi_{\mathbf{q}}\right]^2} \left(4\frac{J''}{J'} - \frac{\varepsilon_B}{J'} - 4\right) \right|^2 \\
A^2 &= \frac{2}{3} \iint_{-\pi}^{\pi} \left| \frac{\left[\frac{\varepsilon_B}{J'} + 4 + 4\xi_{\mathbf{q}}\right]}{\left(\frac{J''}{J'} + \xi_{\mathbf{q}}\right)} \frac{1}{(2\pi)^2} d^2\mathbf{q} \right|^2 \\
0 &= \iint_{-\pi}^{\pi} \frac{\frac{J''}{J'} + \xi_{\mathbf{q}}}{\left[\frac{\varepsilon_B}{J'} + 4 + 4\xi_{\mathbf{q}}\right]} \frac{1}{(2\pi)^2} d^2\mathbf{q}
\end{aligned}$$

Therefore we can solve these equations for each particular value of $\frac{J''}{J'}$ and $\frac{\varepsilon_B}{J'}$ similar to the binding energy plot and then using these values plot $\langle d^2 \rangle$ against the coupling constant. This is plotted in Figure 3.7 for the $\mathbf{Q} = 0, (1.73)$ and $(3, 0)$ singlet channel. This is exactly what we expect to see, as the RMS diameter reflects the spatial extent of the wavefunction in the strong coupling limit (tight binding) we expect a highly localised wavefunction however in the weak coupling regime $\frac{J''}{J'} \to \left(\frac{J''}{J'}\right)_{crit}+$ the wavefunction is very weakly bound and therefore not localised and we have that $D_{RMS} \to \infty$.

3.5.2 Non-Zero Total Momentum

Now we look at the case for a non zero total momentum in the singlet channel. This case is similar to the $\mathbf{Q} = 0$ case except in the dispersion relation we have an extra dependence on the total momentum in the x and y direction. The BSE equation for

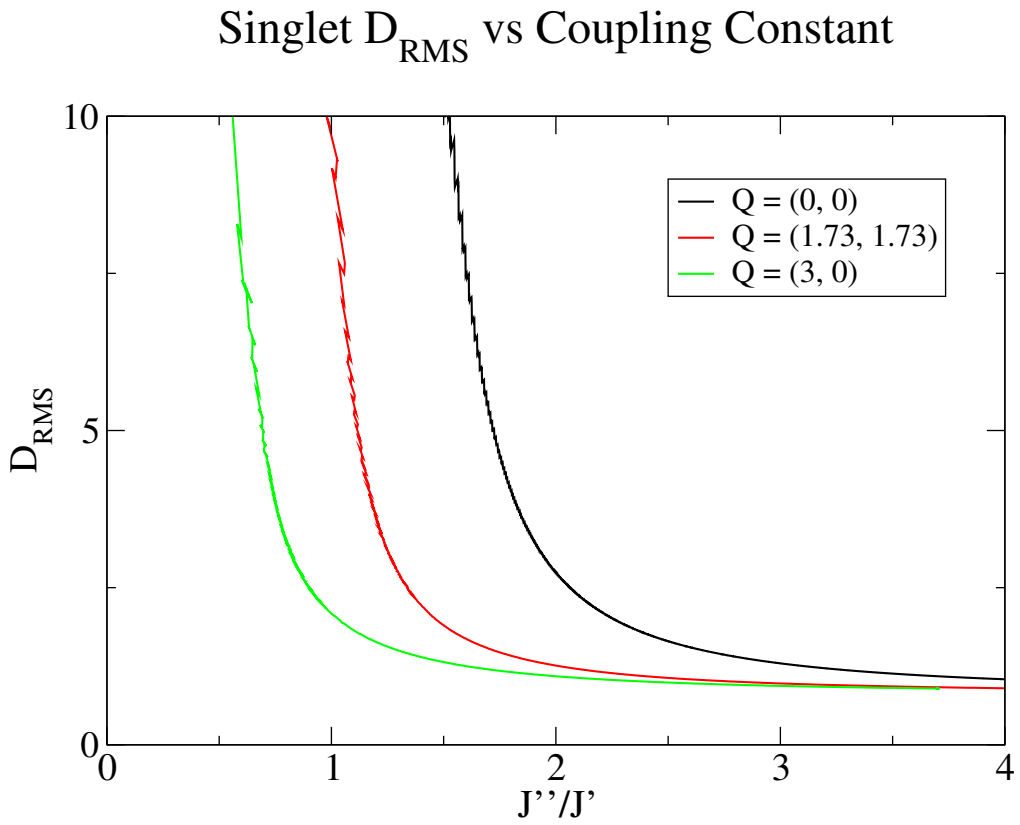

Figure 3.7: RMS diameter of singlet states. This plot shows how the RMS diameter of the wavefunction for three different total momentum is dependent on the coupling constant. This agrees with our prediction that in the strong coupling regime $D_{RMS} \to \frac{J''}{J'}$.

this state is given by (3.19) with the condition (3.21) which we rewrite as,

$$\begin{aligned}
-J'\mathcal{D}'\left(\mathbf{q},\mathbf{Q},\varepsilon_B\right)\psi\left(\mathbf{q}\right) &= \sum_{\mathbf{p}}\left\{-4J''\xi_{\mathbf{q}}\xi_{\mathbf{p}}+2U\right\}\psi\left(\mathbf{p}\right)\\
\Rightarrow \psi\left(\mathbf{q}\right) &= \frac{4J''}{J'}\frac{\xi_{\mathbf{q}}}{\mathcal{D}'\left(\mathbf{q},\mathbf{Q},\varepsilon_B\right)}\sum_{\mathbf{p}}\xi_{\mathbf{p}}\psi\left(\mathbf{p}\right)-\frac{2U}{\mathcal{D}'\left(\mathbf{q},\mathbf{Q},\varepsilon_B\right)}\sum_{\mathbf{p}}\xi_{\mathbf{p}}\psi\left(\mathbf{p}\right)\\
\text{Where } \mathcal{D}'\left(\mathbf{q},\mathbf{Q},\varepsilon_B\right) &= \frac{\varepsilon_B}{J'}+2\left[\cos\left(\frac{Q_x}{2}\right)\left(1+\cos\left(q_x\right)\right)+\cos\left(\frac{Q_y}{2}\right)\left(1+\cos\left(q_y\right)\right)\right].
\end{aligned}$$

Therefore we see that our wavefunction must have the form,

$$\psi\left(\mathbf{q}\right)=A\frac{C+\xi_{\mathbf{q}}}{\mathcal{D}'\left(\mathbf{q},\mathbf{Q},\varepsilon_B\right)}, \tag{3.38}$$

Once again we have to enforce the hardcore constraint,

$$\begin{aligned}
\sum_{\mathbf{q}}\psi\left(\mathbf{q}\right)&=0\\
\Rightarrow \frac{C+\xi_{\mathbf{q}}}{\mathcal{D}'\left(\mathbf{q},\mathbf{Q},\varepsilon_B\right)}&=0
\end{aligned} \tag{3.39}$$

And similar to the $\mathbf{Q}=0$ case we find the relation,

$$\sum_{\mathbf{p}}\xi_{\mathbf{p}}\frac{C+\xi_{\mathbf{p}}}{\mathcal{D}'\left(\mathbf{q},\mathbf{Q},\varepsilon_B\right)}=\frac{J'}{4J''}.$$

Unlike the $\mathbf{Q}=0$ there is no trivial relation between the coupling ratio and the constant C like (3.33). Therefore we have to numerically solve both of these equations "simultaneously". A plot of different total momentum is given below with the $\mathbf{Q}=0$ case for comparison. In general this was a slightly naive calculation as we did not consider the anisotropy of the wavefunction in the $\mathbf{Q}\neq 0$ case which invalidates (3.21) for large $\mathbf{Q}$ but should be a valid approximation for low total momentum.

3.6 Triplet Channel Bound State, S = 1

The triplet case is the second of three possible bound states between the two triplets. The derivation for the form of the case can be found in appendix C.2. From this we see that for some polarisation μ, the Born Amplitude is given by,

$$M_{\mu}^{(1)}\left(\mathbf{q},\mathbf{p}\right)=\frac{1}{2}\epsilon_{\mu\alpha\beta}\epsilon_{\mu\gamma\delta}M_{\alpha\beta,\gamma\delta}\left(\mathbf{q},\mathbf{p}\right).$$

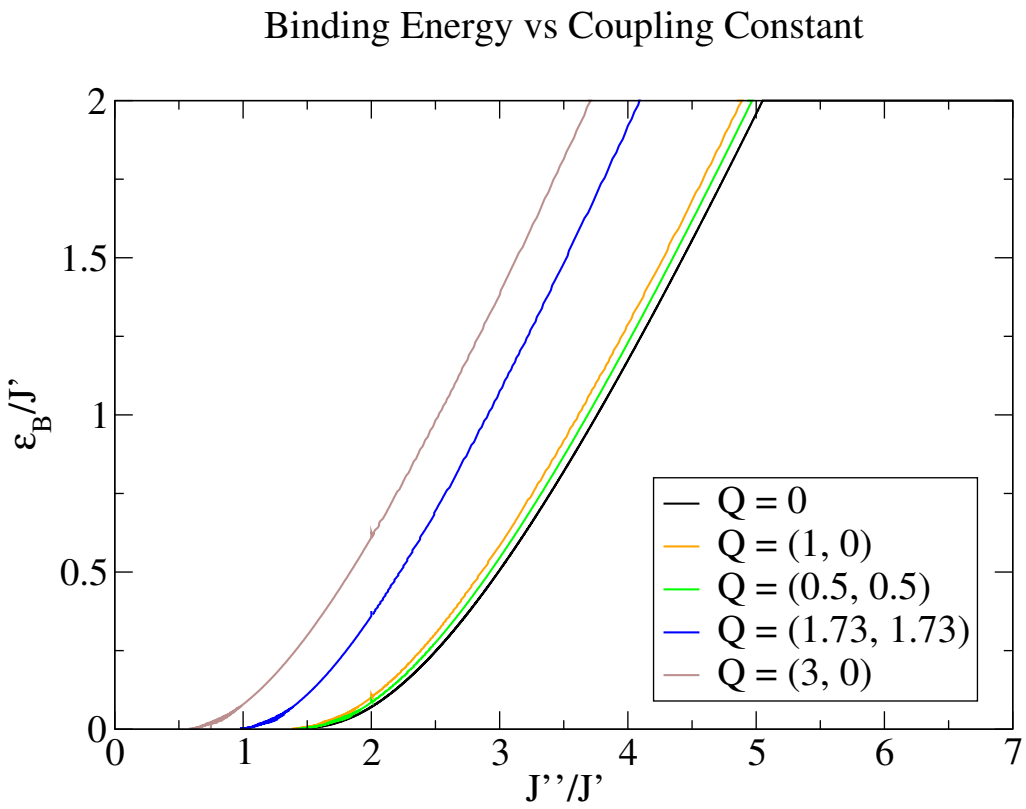

Figure 3.8: Plot of binding energy vs coupling constant for the singlet channel for non zero total momentum. This plot shows how the coupling constant effects the binding energy in the singlet channel. The $\mathbf{Q} = (3, 0)$ and $\mathbf{Q} = (1.73, 1.73)$ show that the greater the total momentum the lower the critical coupling. However from the plot we see that the gradient in the strong coupling regime for all the couplings are approximately the same.

Where there is no implied summation over μ. Therefore we find for (3.13) this triplet channel is given by,

$$M_{\mu}^{(1)}(\mathbf{q},\mathbf{p}) = \frac{1}{2}\epsilon_{\mu\alpha\beta}\epsilon_{\mu\gamma\delta}J''\left[\delta_{\alpha\gamma}\delta_{\beta\delta}+\delta_{\alpha\delta}\delta_{\beta\gamma}-2\delta_{\alpha\beta}\delta_{\gamma\delta}\right](\cos(q_x)\cos(p_x)+\cos(q_y)\cos(p_y))$$
$$-\frac{1}{2}\epsilon_{\mu\alpha\beta}\epsilon_{\mu\gamma\delta}J''\left[\delta_{\alpha\gamma}\delta_{\beta\delta}-\delta_{\alpha\delta}\delta_{\beta\gamma}\right](\sin(q_x)\sin(p_x)+\sin(q_y)\sin(p_y))$$
$$+\frac{1}{2}\epsilon_{\mu\alpha\beta}\epsilon_{\mu\gamma\delta}U\left[\delta_{\alpha\gamma}\delta_{\beta\delta}+\delta_{\alpha\delta}\delta_{\beta\gamma}\right].$$

For some polarisation μ, we have the relations,

$$\epsilon_{\mu\alpha\beta}\epsilon_{\mu\gamma\delta}\delta_{\alpha\beta}\delta_{\gamma\delta} = 0,$$
$$\epsilon_{\mu\alpha\beta}\epsilon_{\mu\gamma\delta}\delta_{\alpha\gamma}\delta_{\beta\delta} = 2,$$
$$\epsilon_{\mu\alpha\beta}\epsilon_{\mu\gamma\delta}\delta_{\alpha\delta}\delta_{\beta\gamma} = -2.$$

Therefore the Born amplitude for the $\mathbf{S=1}$ channel to be,

$$M_{\mu}^{(1)}(\mathbf{p},\mathbf{q}) = -2J''\left[\sin(q_x)\sin(p_x)+\sin(q_y)\sin(p_y)\right].$$

Therefore for the triplet case, the BSE is,

$$\left(E-\varepsilon_{\frac{\mathbf{Q}}{2}+\mathbf{q}}-\varepsilon_{\frac{\mathbf{Q}}{2}+\mathbf{q}}\right)\psi(\mathbf{q}) = \frac{1}{2}\sum_{\mathbf{p}}M_{\mu}^{(1)}(\mathbf{q},\mathbf{p})\,\psi(\mathbf{p}),$$
$$J'\left\{\frac{\varepsilon_B}{J'}+2\left[\cos\left(\frac{Q_x}{2}\right)(1+\cos(q_x))+\cos\left(\frac{Q_y}{2}\right)(1+\cos(q_y))\right]\right\}\psi(\mathbf{q}) =$$
$$\sum_{\mathbf{p}}J''\left[\sin(q_x)\sin(p_x)+\sin(q_y)\sin(p_y)\right]\psi(\mathbf{p}). \qquad (3.40)$$

Unlike the singlet channel we cannot simplify the RHS of (3.40) using the properties of the C_4 point symmetry group as the wavefunction has negative parity.

3.6.1 Zero Total Momentum, Q = 0

Again we consider the simplest case in the triplet channel when there is no total momentum $\mathbf{Q} = 0$. The BSE is given by,

$$\begin{aligned} -J'\left[\frac{\varepsilon_B}{J'} + 4 + 4\xi_{\mathbf{q}}\right]\psi\left(q_x, q_y\right) &= \sum_{\mathbf{p}} -J''\left[\sin\left(q_x\right)\sin\left(p_x\right) + \sin\left(q_y\right)\sin\left(p_y\right)\right]\psi\left(\mathbf{p}\right), \\ \Rightarrow \psi\left(\mathbf{q}\right) = \frac{J''}{J'}\frac{\sin\left(q_x\right)}{\left[\frac{\varepsilon_B}{J'} + 4 + 4\xi_{\mathbf{q}}\right]}\sum_{\mathbf{p}}\sin\left(p_x\right)\psi\left(\mathbf{p}\right) &+ \frac{J''}{J'}\frac{\sin\left(q_y\right)}{\left[\frac{\varepsilon_B}{J'} + 4 + 4\xi_{\mathbf{q}}\right]}\sum_{\mathbf{p}}\sin\left(p_y\right)\psi\left(\mathbf{p}\right). \end{aligned} \tag{3.41}$$

It should be noted that there is no requirement to enforce a hardcore condition in the triplet channel case as there is no diverging term in (3.41). This is because the wavefunction is anti-symmetric and it will be normalised such that there are no triplets on a single lattice site.

From (3.41) we see that the wavefunction is separable into two wavefunctions,

$$\begin{aligned} \psi_x\left(\mathbf{q}\right) &= A\frac{\sin\left(q_x\right)}{\left[\frac{\varepsilon_B}{J'} + 4 + 4\xi_{\mathbf{q}}\right]}, \\ \psi_y\left(\mathbf{q}\right) &= B\frac{\sin\left(q_y\right)}{\left[\frac{\varepsilon_B}{J'} + 4 + 4\xi_{\mathbf{q}}\right]}. \end{aligned} \tag{3.42}$$

and any linear combination of them (in the $\mathbf{Q} = 0$ case $A = B$). Therefore we can see that the triplet case is doubly degenerate in the $\mathbf{Q} = 0$ for each direction. Therefore from this point on we will only consider the properties of the wavefunction in the x direction ψ_x with the understand that it is identical in the y-direction

Therefore substituting (3.42) into (3.41) we have that,

$$\begin{aligned} \sin\left(q_x\right) &= \frac{J''}{J'}\sin\left(q_x\right)\sum_{\mathbf{p}}\frac{\sin^2\left(p_x\right)}{\left[\frac{\varepsilon_B}{J'} + 4 + 4\xi_{\mathbf{p}}\right]}, \\ \Rightarrow \sum_{\mathbf{p}}\frac{\sin^2\left(p_x\right)}{\left[\frac{\varepsilon_B}{J'} + 4 + 4\xi_{\mathbf{p}}\right]} &= \frac{J'}{J''}. \end{aligned} \tag{3.43}$$

Critical Coupling

To find the critical coupling in the triplet case we have to consider the case where the $\varepsilon \to 0$. In this limit (3.43) becomes,

$$\sum_{\mathbf{p}} \frac{\sin^2(p_x)}{4 + 4\xi_{\mathbf{p}}} = \left(\frac{J'}{J''}\right)_{crit}. \tag{3.44}$$

By inspection we see that at the singularity $(p_x, p_y) = (\pi, \pi)$ the numerator is satisfied and therefore the equation is finite for all points as required. To find the critical coupling $\left(\frac{J''}{J'}\right)_{crit}$ such that (3.44) is satisfied we once again have to solve it numerically. Using the method described in appendix D to find the root we find that the critical coupling point is,

$$\left(\frac{J''}{J'}\right)_{crit} \approx 5.5$$

Therefore we immediately see that in the triplet channel a much higher coupling is required to form a bound state than the singlet channel's $\left(\frac{J''}{J'}\right)_{Scrit} = 1$.

Strong Coupling

Similar to the singlet channel, in the strong coupling limit $J'' \gg 1$, where $\varepsilon_B \gg 1$, (3.43) becomes in integral form,

$$\sum_{\mathbf{p}} \frac{\sin^2(p_x)}{\frac{\varepsilon_B}{J'}} = \frac{J'}{J''},$$
$$\int_{-\pi}^{\pi}\int_{-\pi}^{\pi} \frac{\sin^2(p_x)}{\frac{\varepsilon_B}{J'}} \frac{1}{(2\pi)^2} d^2\mathbf{p} = \frac{J'}{J''}.$$

Which gives the analytic solution,

$$\frac{\varepsilon_B}{J'} = \frac{1}{2}\frac{J''}{J'}. \tag{3.45}$$

Comparing this to the singlet channel's strong coupling limit (3.35) we see that for strong coupling the triplet channel is again weaker than the singlet channel however to see this strong coupling relation we have to have a very high coupling $\frac{J''}{J'} \approx 20$ and therefore can not be seen in Figure 3.9.

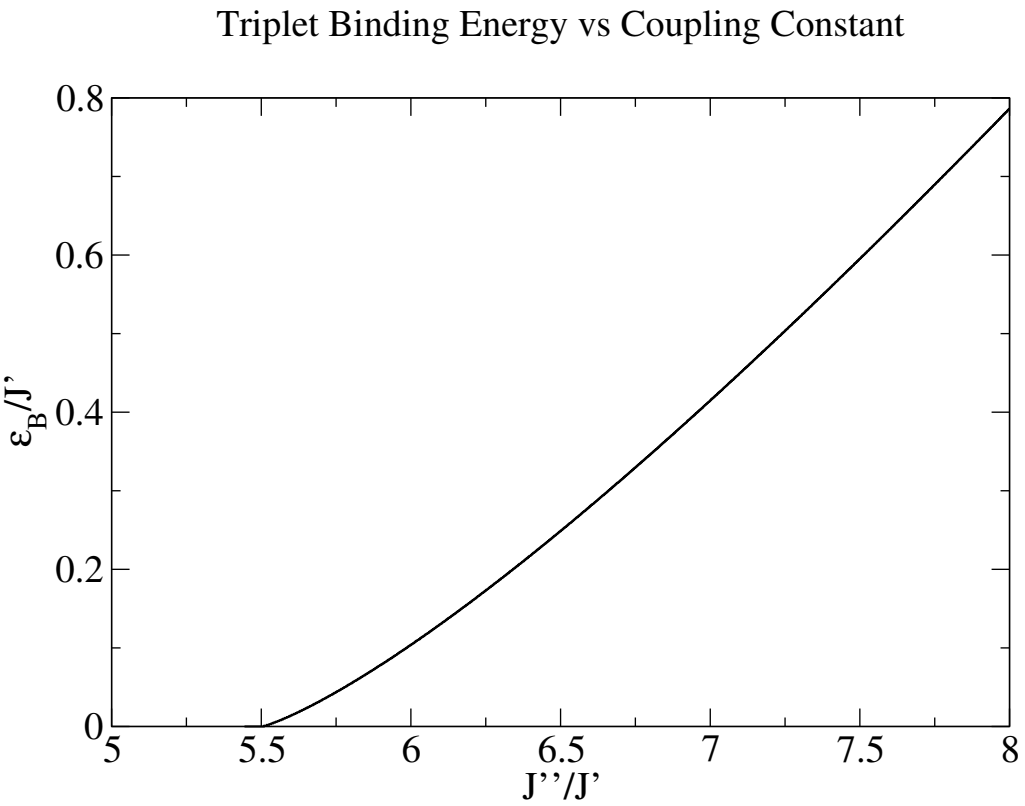

Figure 3.9: Plot of bound state energy vs coupling constant. This shows the numerical plot of how the coupling constant affects the bound state energy in the triplet channel. This shows that for $\frac{J''}{J'} < 5.5$ the bound state does not exist as we calculated in the previous section.

Bound State vs Coupling Constant

Using the method outlined in appendix D and used in the singlet channel case we numerically solve (3.43) and find the roots for corresponding values of the coupling constant ratio. As the critical coupling point $\left(\frac{J''}{J'}\right)_{crit} \approx 5.5$ we plot the relation for $\frac{J''}{J'} \in (5, 8)$ in Figure 3.9.

3.6.2 Non-Zero Total Momentum

The cases where the triplon pair has a total momentum along the lattice are much simpler to solve for the triplet channel. This is because the hard core constraint is inherently contained in the BSE equation and therefore there for there is only one equation to solve. To see this note that in the $\mathbf{Q} \neq 0$ case the BSE equation is given

by (3.40) and therefore can be rewritten as,

$$\mathcal{D}'(\mathbf{q},\mathbf{Q},\varepsilon_B)\,\psi(\mathbf{q}) = \frac{J''}{J'}\sum_{\mathbf{p}}\left[\sin(q_x)\sin(p_x)+\sin(q_y)\sin(p_y)\right]\psi(\mathbf{p}),$$

$$\Rightarrow \psi(\mathbf{q}) = \frac{J''}{J'}\frac{\sin(q_x)}{\mathcal{D}'(\mathbf{q},\mathbf{Q},\varepsilon_B)}\sum_{\mathbf{p}}\sin(p_x)\,\psi(\mathbf{p}) + \frac{J''}{J'}\frac{\sin(q_y)}{\mathcal{D}'(\mathbf{q},\mathbf{Q},\varepsilon_B)}\sum_{\mathbf{p}}\sin(p_y)\,\psi(\mathbf{p}),$$

$$\text{Where } \mathcal{D}'(\mathbf{q},\mathbf{Q},\varepsilon_B) = \frac{\varepsilon_B}{J'}+2\left[\cos\left(\frac{Q_x}{2}\right)(1+\cos(q_x))+\cos\left(\frac{Q_y}{2}\right)(1+\cos(q_y))\right].$$

and therefore similar to the $\mathbf{Q}=0$ the wavefunction and necessary coupling relation are given by,

$$\psi_x(\mathbf{q}) = A\frac{\sin(q_x)}{\mathcal{D}'(\mathbf{q},\mathbf{Q},\varepsilon_B)}, \tag{3.46}$$

$$\psi_y(\mathbf{q}) = B\frac{\sin(q_y)}{\mathcal{D}'(\mathbf{q},\mathbf{Q},\varepsilon_B)},$$

$$\sum_{\mathbf{q}}\frac{\sin^2(q_x)}{\mathcal{D}'(\mathbf{q},\mathbf{Q},\varepsilon_B)} = \frac{J'}{J''}, \tag{3.47}$$

$$\sum_{\mathbf{q}}\frac{\sin^2(q_y)}{\mathcal{D}'(\mathbf{q},\mathbf{Q},\varepsilon_B)} = \frac{J'}{J''}. \tag{3.48}$$

Once again in the triplet case we have two separate wavefunctions and conditions for the x and y directions. Therefore for the remainder of this section we consider only the x-direction with the understanding that in the y-direction there is a similar answer. We will see however that due to anisotropy of the total momentum the degeneracy of the system is lifted.

Now we can numerically solve the coupling relation (3.47) for a particular $\mathbf{Q}$ to find both the critical coupling and the plot of binding energy vs coupling constant. Like the singlet channel the strong coupling state is identical to the $\mathbf{Q}=0$ case (3.45). Therefore in order to compare effectively with the singlet channel we plot the same cases as the singlet channel for comparison Figure 3.10, however in this case to demonstrate the anisotropy of the total momentum we need to plot (Q_x,Q_y) and (Q_y,Q_x).

Therefore we see that compared to the singlet channel the anisotropy of the total momentum produces large a discrepancy in the binding energy. Superficially this looks like the system breaks rotational invariance however due to the antisymmetric proper-

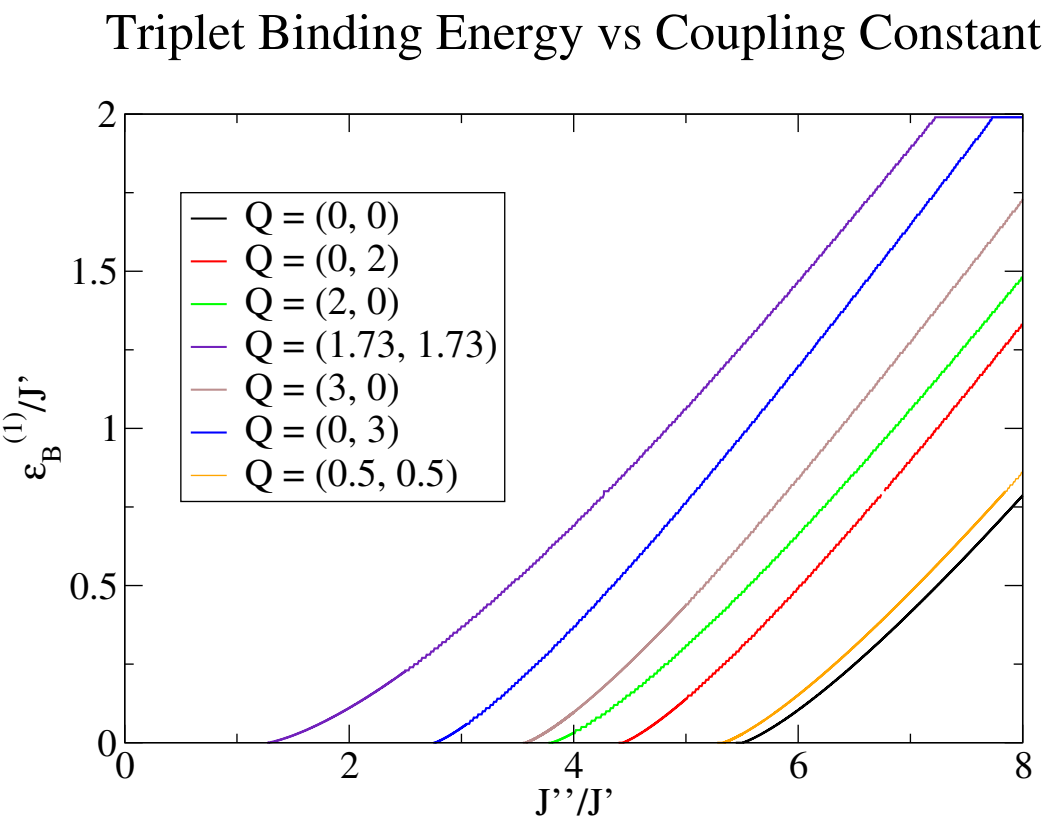

Figure 3.10: Triplet Bound state for various total momenta for the x-direction (in the y-direction the plots are identical except with the permutation $(Q_x, Q_y) \to (Q_y, Q_x)$). This plot shows how the binding energy depends on the coupling constant for $\mathbf{Q} = (0,0), (0.5, 0.5),$
$(2,0), (0,2), (3,0), (0,3), (1.73, 1.73)$. As you can see the anisotropy of the total momentum effects the triplets states more than the singlet states in Figure 3.8.

ties of the triplet wavefunction which means that the wavefunction can be split into x and y directions and therefore both of these bound states exists one in each direction and therefore under a rotation of 90° the two states "flip" directions but not net difference and therefore the system is invariant in the triplet channel that is under rotation.

3.7 Triplet Channel RMS Diameter

For the triplet channel we also find the RMS diameter of the wavefunction. From Appendix C.1 we have that the normalisation of the triplet channel is $P^2 = 2$, and therefore using the wavefunction (3.42) we have from (3.15) that the normalisation constant of the wavefunction in the x-direction is given by,

$$A^2 = \sum_{\mathbf{q}} \left| \frac{\frac{\varepsilon_B}{J'} + 4 + 4\xi_{\mathbf{q}}}{\sin(q_x)} \right|^2$$

and therefore from (3.16) we have we find that,

$$\langle d^2 \rangle = A^2 \sum_{\mathbf{q}} \left| \frac{\left[\cos(q_x)\,\mathcal{D}(\mathbf{q}, \varepsilon_B) + \sin(q_x)\cos(q_x) + \sin(q_x)\cos(q_y)\right]}{\mathcal{D}(\mathbf{q}, \varepsilon_B)^2} \right|^2 .$$

$$R_{RMS} = \sqrt{\langle d^2 \rangle}$$

Therefore from these along with the coupling condition (3.43) we find the triplet state RMS for the $\mathbf{Q} = 0$ wavefunction. Similarly with the Non-Zero case the normalisation constant and RMS wavefunction we have the similar conditions,

$$A^2 = \sum_{\mathbf{q}} \left| \frac{\mathcal{D}'(\mathbf{q}, \mathbf{Q}, \varepsilon_B)}{\sin(q_x)} \right|^2$$

$$\langle d^2 \rangle = A^2 \sum_{\mathbf{q}} \left| \frac{\left[\cos(q_x)\,\mathcal{D}'(\mathbf{q}, \mathbf{Q}, \varepsilon_B) + 2\sin(q_x)\left(\cos\left(\frac{Q_x}{2}\right)\sin(q_x) + \cos\left(\frac{Q_y}{2}\right)\sin(q_y)\right)\right]}{\mathcal{D}'(\mathbf{q}, \mathbf{Q}, \varepsilon_B)^2} \right|^2$$

Therefore solving this numerically we plot the RMS case in Figure 3.11 for the total momenta $\mathbf{Q} = (1.73, 1.73), (3, 0), (0, 0)$ and $(0, 3)$ to demonstrate the anisotropy of the RMS diameter.

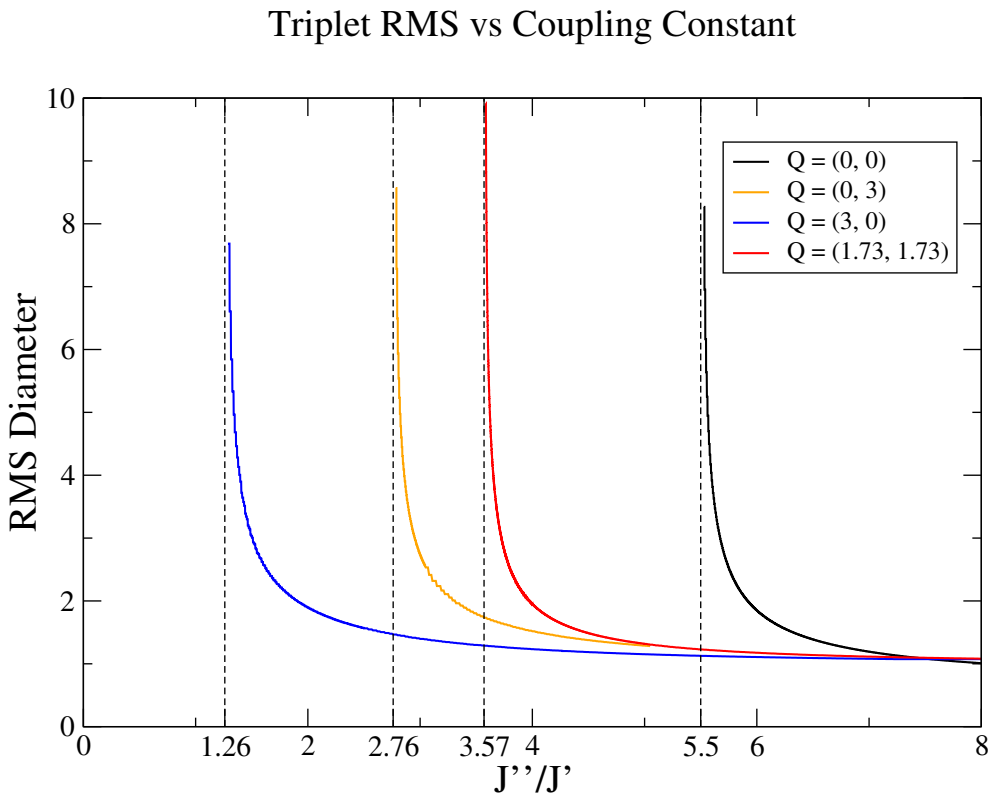

Figure 3.11: Plot of three RMS diameters for the triplet channel for different total momentum. As plotted the RMS diameter is asymptotic as it approaches the critical coupling for the various momenta as the state is weakly bou and therefore not localised. Also the RMS diameters approach 1 in the strong coupling regime as the bound states become heavily localised on the bilayer and is only bounded by the lattice spacing (in our case unity).

3.8 Quadrupole Channel Bound State, S = 2

We now consider the last possible spin channel, the quadrupole channel. The derivation of the quadrupole channel can be found in appendix C.3. From this we find that Born amplitude in the quadrupole channel for a particular polarisation S_{xy} is given by,

$$M^{(2)} = \frac{1}{2}\left(\delta_{x\gamma}\delta_{y\delta} + \delta_{x\delta}\delta_{y\gamma}\right) M_{\alpha\beta,\gamma\delta}\left(\delta_{x\alpha}\delta_{y\beta} + \delta_{x\beta}\delta_{y\alpha}\right)$$

and therefore,

$$\begin{aligned} M^{(2)} = \frac{1}{2}\left(\delta_{x\alpha}\delta_{y\beta} + \delta_{x\beta}\delta_{y\alpha}\right)\left(\delta_{x\gamma}\delta_{y\delta} + \delta_{x\delta}\delta_{y\gamma}\right) \times \\ J''\left[\delta_{\alpha\gamma}\delta_{\beta\delta} + \delta_{\alpha\delta}\delta_{\beta\gamma} - 2\delta_{\alpha\beta}\delta_{\gamma\delta}\right]\left(\cos\left(q_x\right)\cos\left(p_x\right) + \cos\left(q_y\right)\cos\left(p_y\right)\right) \\ -\frac{1}{2}\left(\delta_{x\alpha}\delta_{y\beta} + \delta_{x\beta}\delta_{y\alpha}\right)\left(\delta_{x\gamma}\delta_{y\delta} + \delta_{x\delta}\delta_{y\gamma}\right) \times \\ J''\left[\delta_{\alpha\gamma}\delta_{\beta\delta} - \delta_{\alpha\delta}\delta_{\beta\gamma}\right]\left(\sin\left(q_x\right)\sin\left(p_x\right) + \sin\left(q_y\right)\sin\left(p_y\right)\right) \\ +\frac{1}{2}\left(\delta_{x\alpha}\delta_{y\beta} + \delta_{x\beta}\delta_{y\alpha}\right)\left(\delta_{x\gamma}\delta_{y\delta} + \delta_{x\delta}\delta_{y\gamma}\right) U\left[\delta_{\alpha\gamma}\delta_{\beta\delta} + \delta_{\alpha\delta}\delta_{\beta\gamma}\right]. \end{aligned}$$

After completing the summation we are left with the Born amplitude,

$$M^{(2)} = 2J''\left(\cos\left(q_x\right)\cos\left(p_x\right) + \cos\left(q_y\right)\cos\left(p_y\right)\right) + 2U$$

However, as the amplitude is positive the channel is repulsive. Therefore no bound states can form in the quadrupole channel.

3.9 Summary of Triplon Bound States

In this chapter we developed and implemented a process for finding the properties of a two triplon bound state for the AFM bilayer. The bound state is an important property especially for further study especially in the context of a triplon condensate as we will discuss in chapter 3. Therefore it is important to find the most practical and effective bound state. Comparing the singlet and triplet and quadrupole channels we see there are clear distinctions in their bound states, and in the case of the quadrupole there is no bound state and therefore we will not consider it.

Overall it is much easier to form a bound state in the singlet channel than the triplet channel. To see this we ultimately have to compare the singlet (Figure 3.8) and triplet (Figure 3.10) bound states for different total momenta. We see that the singlet case consistently has a much lower critical coupling than the triplet case and therefore it is much easy to initially form a bound state. Most importantly however is the magnitude of the bound state for similar coupling. Considering both plots we see that in the singlet channel the binding energy is much larger for the same coupling constant. In the strong coupling regime we found from equation 3.35 and 3.45 that the singlet binding energy is $\frac{J''}{J'} \approx 2$ times greater than the triplet channel in the $\mathbf{Q} = 0$ case. Also in the $\mathbf{Q} = 0$ case the singlet channel has a unitless binding energy of $\frac{\varepsilon_B}{J'} \approx 2$ at a coupling of $\left(\frac{J''}{J'}\right)_{crit} \approx 5$ before the triplet channel has any bound state.

Chapter 4

Conclusion and Discussion

In this chapter we will present an overview of the results of the thesis and discuss future work and possibilities.

4.1 Summary of Results

In this thesis we have considered important properties of a topical model in quantum magnetism and Condensed matter physics. In chapter 2 we introduced the AFM bilayer model which describes the formation of the quantum fluctuations at absolute zero and from these show the presence of a QPT when using the coupling constant as a tuning parameter and found the existence of a spin gap for triplon excitations and more importantly the dispersion relation for triplons in the highly disordered regime where we found the bound states.

Using the Bethe-Salpeter equation in chapter 3 and the dispersion relation of the triplon excitations we found properties of the bound state of two triplons in the highly disordered regime for the three different channels and how these bound states depend on the coupling of the system. The three channels represent different spin polarisations of the two triplons, where we found that the singlet channel ($S = 0$) and triplet channel ($S = 1$) can both support bound states due to the attractive interaction however the quadrapole channel ($S = 2$) is repulsive and no bound states exist, therefore we only consider the triplet and singlet channels.

In the formation of bound states the most important property is the critical value for bound states can form. In this model this is the ratio $\frac{J''}{J'}$ such that $\frac{\varepsilon_B}{J'} > 0$. Com-

paring Figure 3.8 and Figure 3.10 we found that in the singlet channel the critical coupling consistently lower than the triplet channel.

Another important property we discovered was the robustness of the bound state in the two channels. Once again comparing the two plots of the bound states vs coupling constant (Figure 3.8 and Figure 3.10) we saw that for a particular coupling constant the singlet channel bound state is consistently greater and therefore the singlet channel has the most robust bound state.

The final property we found from the two valid channels is localisation of the bound states in the RMS diameter in Figure 3.7 and Figure 3.11. The RMS diameter is intimately related to the bound state of the system as weakly bound states (low ε_B) are not localised and therefore have a large RMS whereas in the strong coupling regime the bound state is highly localised and has a small RMS. Therefore as the singlet channel is more robust and has a lower critical coupling than the RMS diameter will be smaller than the triplet channel for similar momenta. This will be an important factor when considering the interaction of two bound states (next section).

Therefore in consideration of these factors we see that the singlet channel is much more favourable for the formation of a bound state than the other two channels. Therefore with this basis we can now consider future directions for the applications of these bound states.

4.2 Outlook and Future Research

This research has provided a solid foundation for further research into the behaviour of triplons in the disordered dimer phase. The bound state of quasi-particles is a natural first step in the direction of the formation of a macroscopic condensate of the quasi-particles, the most salient case being that of a cooper pair formed from the bound state of two electrons [15] and then the condensation of these Cooper pairs produces the non dissipative superconductive state described by BCS theory [4]. In the context of quantum magnetism, there has been topical research into the existence of condensates of magnon quasi-particles [53][54] including a recent review in modern physics [55].

As we have found the bound states of triplon in the disordered phase of the AFM bilayer the next step will be to find how these bound states interact and if there exists

a condensate of triplons in our system. Given the nature of the disordered regime and the vanishing viscosity of the BEC state (like in He_4) we believe that if the triplons do condense the state will behave as a spin liquid [14].

As discussed in the introduction the theoretical derivation of this spin liquid could have a large impact on the field of condensed matter due to its connection to the elusive HTSC state. As the bilayer layer model is an possible approximation to certain layered cuprates which exhibit HTSC [44, 37, 45, 46] the triplon bound state and resulting condensate could have a far reaching implications.

Appendix A

Boson Commutation Relations

In this thesis we use a second quantisation bond operator approach to describe the Hamiltonian of the AFM bilayer. A bond operator for each lattice point i describes two electrons in the bilayer which together have spin 0 or 1 and therefore together act as boson. Therefore the bond operators must satisfy the bosonic commutation relations. That is for for two boson operators $b_{\mathbf{k}}$ and $b_{\mathbf{l}}$ the following must hold,

$$\begin{aligned} \left[b^{\dagger}_{\mathbf{k}}, b^{\dagger}_{\mathbf{l}}\right] = [b_{\mathbf{k}}, b_{\mathbf{l}}] = 0 \\ \left[b_{\mathbf{k}}, b^{\dagger}_{\mathbf{l}}\right] = \delta_{\mathbf{kl}} \end{aligned}$$

and therefore the Bogoliubov transform must also obey the conditions,

$$\begin{aligned} \beta_{\mathbf{k}} &= u_{\mathbf{k}} b_{\mathbf{k}} + v_{\mathbf{k}} b^{\dagger}_{-\mathbf{k}}, \\ \beta^{\dagger}_{\mathbf{k}} &= u_{\mathbf{k}} b^{\dagger}_{\mathbf{k}} + v_{\mathbf{k}} b_{-\mathbf{k}}, \\ \Rightarrow \left[\beta_{\mathbf{k}}, \beta^{\dagger}_{\mathbf{k}}\right] &= \left[u_{\mathbf{k}} b_{\mathbf{k}} + v_{\mathbf{k}} b^{\dagger}_{-\mathbf{k}}, u_{\mathbf{k}} b^{\dagger}_{\mathbf{k}} + v_{\mathbf{k}} b_{-\mathbf{k}}\right], \\ &= u^2_k \left[b_{\mathbf{k}}, b^{\dagger}_{\mathbf{k}}\right] + v^2_{\mathbf{k}} \left[b^{\dagger}_{-\mathbf{k}}, b_{-\mathbf{k}}\right], \\ &= u^2_{\mathbf{k}} - v^2_{\mathbf{k}}. \end{aligned}$$

Therefore as the Bogoliubov operators are also bosons we have that,

$$\begin{aligned} \left[\beta_{\mathbf{k}}, \beta_{\mathbf{k}}^{\dagger}\right] &= 1, \\ \Rightarrow u_{\mathbf{k}}^2 - v_{\mathbf{k}}^2 &= 1, \\ \Rightarrow u_{\mathbf{k}} &= \cosh(\theta), \\ v_{\mathbf{k}} &= \sinh(\theta). \end{aligned}$$

In this representation θ represents a rotation through an imaginary angel in the space of the Bogoliubov transform [15].

Appendix B

Heisenberg to Bond Operators Calculation

In this appendix I will show how the bond operator approach perfectly maps the Heisenberg Hamiltonian to the effective Hamiltonian for triplet excitations used in the AFM bilayer model. The Heisenberg Hamiltonian for the unfrustrated AMF bilayer is given by,

$$H = J_{\parallel} \sum_{\langle i,j \rangle} (\mathbf{S}_{1,i} \cdot \mathbf{S}_{1,j} + \mathbf{S}_{2,i} \cdot \mathbf{S}_{2,j}) + J_{\perp} \sum_{i} \mathbf{S}_{1,i} \cdot \mathbf{S}_{2,i}.$$

Therefore using the bond operators for singlets and triplets from [39],

$$\hat{S}_1^{\alpha} = \frac{1}{2} \left[s^{\dagger} t_{\alpha} + t_{\alpha}^{\dagger} s - i\epsilon_{\alpha\beta\gamma} t_{\beta}^{\dagger} t_{\gamma} \right], \tag{B.1}$$

$$\hat{S}_2^{\alpha} = -\frac{1}{2} \left[s^{\dagger} t_{\alpha} + t_{\alpha}^{\dagger} s + i\epsilon_{\alpha\beta\gamma} t_{\beta}^{\dagger} t_{\gamma} \right], \tag{B.2}$$

where α is the polarisation of the pair, we substitute these operators into the terms of the Heisenberg and separate the order of the triplet operator.

B.1 Parallel Coupling

First we consider the intralayer coupling terms,

$$H_{intra-} = J_{\parallel} \sum_{\langle i,j \rangle} (\mathbf{S}_{1,i} \cdot \mathbf{S}_{1,j} + \mathbf{S}_{2,i} \cdot \mathbf{S}_{2,j}) .$$

Therefore substituting in (B.1), assuming that the ith lattice site has spin polarisation α and the jth site has the polarisation β. We have that (suppressing summation over lattice sites),

$$H_{intra-} = \frac{J_\parallel}{4}\left(s^\dagger_{\alpha,i}t_{\alpha,i} + t^\dagger_{\alpha,i}s_i + i\epsilon_{\alpha\gamma\delta}t^\dagger_{\gamma,i}t_{\delta,i}\right)\left(s^\dagger_{\beta,j}t_{\beta,j} + t^\dagger_{\beta,j}s_{\beta,j} + i\epsilon_{\beta\gamma\delta}t^\dagger_{\gamma,j}t_{\delta,j}\right) + \frac{J_\parallel}{4}\left(s^\dagger_{\alpha,j}t_{\beta,j} + t^\dagger_{\alpha,i}s_{\alpha,i} - i\epsilon_{\alpha\gamma\delta}t^\dagger_{\gamma,i}t_{\delta,i}\right)\left(s^\dagger_{\beta,j}t_{\beta,j} + t^\dagger_{\beta,j}s_{\beta,j} - i\epsilon_{\beta\gamma\delta}t^\dagger_{\gamma,j}t_{\delta,j}\right).$$

Therefore as we are looking for the Hamiltonian for the triplet excitation we no longer consider the singlet operator. Expanding out the above function gives us,

$$H_{intra-} = \frac{J_\parallel}{2}\left(t_{\alpha,i}t_{\beta,j} + t^\dagger_{\beta,j}t_{\alpha,i} + t^\dagger_{\alpha,i}t_{\beta,j} + t^\dagger_{\alpha,i}t^\dagger_{\beta,j}\right) - \frac{J_\parallel}{2}\epsilon_{\alpha\gamma\delta}\epsilon_{\beta\gamma\delta}t^\dagger_{\gamma,i}t_{\delta,i}t^\dagger_{\gamma,j}t_{\delta,j}.$$

Therefore we can split this up into orders of triplet operators,

$$\begin{aligned} H_{intra-,2} &= \frac{J_\parallel}{2}\left(t_{\alpha,i}t_{\beta,j} + t^\dagger_{\beta,j}t_{\alpha,i} + t^\dagger_{\alpha,i}t_{\beta,j} + t^\dagger_{\alpha,i}t^\dagger_{\beta,j}\right), \\ H_{intra-,3} &= 0, \\ H_{intra-,4} &= -\frac{J_\parallel}{2}\epsilon_{\alpha\gamma\delta}\epsilon_{\beta\gamma\delta}t^\dagger_{\gamma,i}t_{\delta,i}t^\dagger_{\gamma,j}t_{\delta,j}, \\ &= \frac{J_\parallel}{2}\left(t^\dagger_{\alpha i}t^\dagger_{\beta,j}t_{\beta,i}t_{\alpha,j} - t^\dagger_{\alpha i}t^\dagger_{\alpha,j}t_{\beta,i}t_{\beta,j}\right). \end{aligned} \tag{B.3}$$

B.2 Perpendicular Coupling

Also for the term in the Heisenberg Hamiltonian that corresponds to the inter-layer coupling,

$$H_{inter-} = J_\perp \sum_i \mathbf{S}_{1,i}\cdot\mathbf{S}_{2,i}.$$

Therefore substituting in the bond operators (B.1) the interlayer coupling term becomes,

$$\begin{aligned} H_{inter-} &= -\frac{J_\perp}{4}\left(s^\dagger_{\alpha,i}t_{\alpha,i} + t^\dagger_{\alpha,i}s_i - i\epsilon_{\alpha\beta\gamma}t^\dagger_{\beta,i}t_{\gamma,i}\right)\left(s^\dagger_{\alpha,j}t_{\alpha,j} + t^\dagger_{\alpha,i}s_{\alpha,i} + i\epsilon_{\alpha\beta\gamma}t^\dagger_{\alpha,i}t_{\alpha,i}\right), \\ &= -\frac{J_\perp}{4}\left[t_{\alpha,i}t_{\alpha,i} + t_{\alpha,i}t^\dagger_{\alpha,i} + t^\dagger_{\alpha,i}t_{\alpha,i} + t^\dagger_{\alpha,i}t^\dagger_{\alpha,i}\right] - \frac{J_\perp}{4}\epsilon_{\alpha\beta\gamma}t^\dagger_{\beta,i}t_{\gamma,i}\epsilon_{\alpha\beta\gamma}t^\dagger_{\beta,i}t_{\gamma,i}. \end{aligned}$$

Splitting this up into orders of triplons,

$$\begin{aligned} H_{inter-,2} &= -\frac{J_\perp}{4}\left(t_{\alpha,i}t_{\alpha,i} + t^\dagger_{\alpha,i}t_{\alpha,i} + t^\dagger_{\alpha,i}t_{\alpha,i} + t^\dagger_{\alpha,i}t^\dagger_{\alpha,i}\right), \\ H_{inter-,3} &= 0, \\ H_{inter-,4} &= \frac{J_\perp}{4}\left(\epsilon_{\alpha\beta\gamma}t^\dagger_{\beta,i}t_{\gamma,i}\epsilon_{\alpha\beta\gamma}t^\dagger_{\beta,i}t_{\gamma,i}\right). \\ &= 0 \end{aligned} \tag{B.4}$$

B.3 Diagonal Coupling (Frustration)

In chapter 3 we introduce a frustration term to determine the bound states. The Heisenberg Hamiltonian for this frustration terms is given by,

$$H_F = J_F \sum_{\langle i,j\rangle} \mathbf{S}_{1,i}\cdot\mathbf{S}_{2,j} + \mathbf{S}_{2,i}\cdot\mathbf{S}_{1,j}.$$

Therefore applying the bond operators (B.1), where the adjacent sites have different polarisations like in the parallel case, the Hamiltonian of the frustration term becomes,

$$\begin{aligned} H_F = &-\frac{J_F}{4}\left(s^\dagger_{\alpha,i}t_{\alpha,i} + t^\dagger_{\alpha,i}s_i - i\epsilon_{\alpha\gamma\delta}t^\dagger_{\gamma,i}t_{\delta,i}\right)\left(s^\dagger_{\beta,j}t_{\beta,j} + t^\dagger_{\beta,j}s_{\beta,j} + i\epsilon_{\beta\gamma\delta}t^\dagger_{\gamma,j}t_{\delta,j}\right) - \\ &\frac{J_F}{4}\left(s^\dagger_{\alpha,j}t_{\beta,j} + t^\dagger_{\alpha,i}s_{\alpha,i} + i\epsilon_{\alpha\gamma\delta}t^\dagger_{\gamma,i}t_{\delta,i}\right)\left(s^\dagger_{\beta,j}t_{\beta,j} + t^\dagger_{\beta,j}s_{\beta,j} - i\epsilon_{\beta\gamma\delta}t^\dagger_{\gamma,j}t_{\delta,j}\right), \\ = &-\frac{J_F}{2}\left(t_{\alpha,i}t_{\beta,j} + t^\dagger_{\beta,j}t_{\alpha,i} + t^\dagger_{\alpha,i}t_{\beta,j} + t^\dagger_{\alpha,i}t^\dagger_{\beta,j}\right) - \frac{J_F}{2}\epsilon_{\alpha\gamma\delta}\epsilon_{\beta\gamma\delta}t^\dagger_{\gamma,i}t_{\delta,i}t^\dagger_{\gamma,j}t_{\delta,j}. \end{aligned}$$

Therefore separating into orders we see that,

$$\begin{aligned} H_{Frust,2} &= -\frac{J_F}{2}\left(t_{\alpha,i}t_{\beta,j} + t^\dagger_{\beta,j}t_{\alpha,i} + t^\dagger_{\alpha,i}t_{\beta,j} + t^\dagger_{\alpha,i}t^\dagger_{\beta,j}\right), \\ H_{Frust,3} &= 0, \\ H_{Frust,4} &= -\frac{J_F}{2}\epsilon_{\alpha\gamma\delta}\epsilon_{\beta\gamma\delta}t^\dagger_{\gamma,i}t_{\delta,i}t^\dagger_{\gamma,j}t_{\delta,j}, \\ &= \frac{J_F}{2}\left(t^\dagger_{\alpha i}t^\dagger_{\beta,j}t_{\beta,i}t_{\alpha,j} - t^\dagger_{\alpha i}t^\dagger_{\alpha,j}t_{\beta,i}t_{\beta,j}\right), \end{aligned} \tag{B.5}$$

B.4 Effective Hamiltonian

To get the effective Hamiltonian of the system (including frustration) we just sum up the all three terms in (B.3), (B.4) and (B.5). Therefore we have,

$$\begin{aligned} H_2 &= \frac{J_{\parallel} - J_F}{2}\left(t_{\alpha,i}t_{\beta,j} + t^{\dagger}_{\beta,j}t_{\alpha,i} + t^{\dagger}_{\alpha,i}t_{\beta,j} + t^{\dagger}_{\alpha,i}t^{\dagger}_{\beta,j}\right) \\ &\quad - \frac{J_{\perp}}{4}\left(t_{\alpha,i}t_{\alpha,i} + t^{\dagger}_{\alpha,i}t_{\alpha,i} + t^{\dagger}_{\alpha,i}t_{\alpha,i} + t^{\dagger}_{\alpha,i}t^{\dagger}_{\alpha,i}\right) \\ H_3 &= 0 \\ H_4 &= \frac{J_{\parallel} + J_F}{2}\left(t^{\dagger}_{\alpha i}t^{\dagger}_{\beta,j}t_{\beta,i}t_{\alpha,j} - t^{\dagger}_{\alpha i}t^{\dagger}_{\alpha,j}t_{\beta,i}t_{\beta,j}\right) \end{aligned} \tag{B.6}$$

Appendix C

Spin Scattering Channels

In the scattering of particles we need to conserve the total spin of the system. This limits the number of possible scattering processes into "spin channels". In the bound state of two triplons, there are 3 possible scattering channels, the singlet ($S = 0$) channel which in analogous to the s-wave state, the triplet ($S = 1$) channel (p-wave state) and the quadrupole ($S = 2$) channel (d-wave). The bound state will have different properties (refer to chapter 3) for different channels and therefore we need to find their influence on the Born amplitude and the wavefunction. In this appendix we suppress momentum and only include the necessary spin notation, the momentum dependence on the channel wavefunction is contained in $\psi(\mathbf{q})$ which is dependent on the relative momentum and total momentum of the triplon pair (3.10). In this appendix we assume that the momentum wavefunction is normalised,

$$|\psi(\mathbf{q})|^2 = 1.$$

In both the initial and final states of the scattering, the wavefunction is the product of two creation operators. These creation operators are elements of the O(3) group,

$$t_\alpha^\dagger \in O(3).$$

Therefore for the bound state we have to consider the tensor product of the group,

$$\tau_{\alpha\beta} = t_\alpha^\dagger t_\beta^\dagger \in \mathrm{O}(3) \otimes \mathrm{O}(3).$$

Therefore our wavefunctions can be represented as a rank 2 tensor $\tau_{\alpha,\beta}$. This is very similar to the standard quantum mechanical representation of angular momentum [56] and therefore we approach it in a similar way.

We can decompose this rank 2 tensor into 3 irreducible components. Initially $\tau_{\alpha,\beta}$ has 9 elements. We decompose it into a scalar component ($T_{\alpha\beta}$), anti-symmetric vector component ($A_{\alpha\beta}$) and a traceless symmetric rank 2 tensor component ($S_{\alpha\beta}$).

$$\tau_{\alpha,\beta} = \frac{1}{3}\delta_{\alpha\beta}\tau_{\alpha\beta} + \frac{(\tau_{\alpha\beta} - \tau_{\beta\alpha})}{2} + \left[\frac{(\tau_{\alpha\beta} + \tau_{\beta\alpha})}{2} - \frac{1}{3}\delta_{\alpha\beta}\tau_{\alpha\beta}\right], \tag{C.1}$$

$$= T_{\alpha\beta} + A_{\alpha\beta} + S_{\alpha\beta}. \tag{C.2}$$

Each of these individual components are closed under spacial rotation and it conserves the number of elements of the original tensor.

$$3 \times 3 = 1 + 3 + 5.$$

C.1 Singlet Channel, S = 0

The singlet channel corresponds to the scalar component or trace of the original tensor in (C.1)

$$T_{\alpha\beta} = \frac{1}{3}\delta_{\alpha\beta}\tau_{\alpha\beta}.$$

Physically it represents the unpolarised spin state which is the average of all possible total polarisations. Therefore it has only 1 component. Now consider an initial wavefunction of our system for the singlet channel,

$$|\psi_i\rangle = P\psi_i(q)\frac{1}{3}\delta_{\alpha\beta}t_\alpha^\dagger t_\beta^\dagger |0\rangle .$$

Where P is some normalisation constant for the channel. To find this normalisation constant we need to satisfy,

$$\begin{aligned} \langle\psi_i | \psi_i\rangle &= 1, \\ \Rightarrow 1 &= \frac{P^2}{4}|\psi(\mathbf{q})|^2 \delta_{\alpha\beta}\delta_{\alpha\beta}\left\langle 0 \middle| t_\beta t_\alpha t_\beta^\dagger t_\alpha^\dagger \middle| 0\right\rangle, \\ \Rightarrow P &= \sqrt{3}. \end{aligned}$$

Therefore the initial wavefunction is given by,

$$|\psi_i\rangle = \frac{1}{\sqrt{3}}\psi_i\left(q\right)\delta_{\alpha\beta}t^\dagger_\beta t^\dagger_\alpha\left|0\right\rangle.$$

Similarly the final state is given by,

$$|\psi_f\rangle = \frac{1}{\sqrt{3}}\psi_f\left(q'\right)\delta_{\gamma\delta}t^\dagger_\gamma t^\dagger_\delta\left|0\right\rangle.$$

Therefore the singlet channel in the first order Born approximation of some Hamiltonian, H is given by,

$$\begin{aligned} M^{(0)}\left(q,q'\right) &= \langle\psi_f\left|\, M_{\alpha\beta,\gamma\delta}\,\right|\psi_i\rangle, \\ &= \frac{1}{3}\delta_{\alpha\beta}\delta_{\gamma\delta}M_{\alpha\beta,\gamma\delta}, \end{aligned}$$

and the square of the normalisation constant for this channel is $P^2 = 3$.

C.2 Triplet Channel, S = 1

The triplet scattering channel corresponds to a bound state with a polarised scattering channel. It is represented by the anti-symmetric component in (C.1),

$$A_{\alpha\beta} = \frac{\left(\tau_{\alpha\beta} - \tau_{\beta\alpha}\right)}{2}.$$

This can be represented in terms of the totally antisymmetric tensor,

$$A_{\alpha\beta} = \frac{1}{2}\epsilon_{\mu\alpha\beta}\tau_{\alpha\beta}. \tag{C.3}$$

With no implied summation over μ (C.3), this corresponds to the spatial polarisation for $\mu = x, y, z$. Similar to the singlet channel we see that the initial wavefunction of the triplet channel is,

$$|\psi_i\rangle = \frac{P}{2}\psi_i\left(\mathbf{q}\right)\epsilon_{\mu\alpha\beta}t^\dagger_\alpha t^\dagger_\beta\left|0\right\rangle.$$

Normalising this wavefunction gives,

$$\begin{aligned} P &= \sqrt{2}, \\ \Rightarrow |\psi_i\rangle &= \frac{1}{\sqrt{2}}\psi_i\left(\mathbf{q}\right)\epsilon_{\mu\alpha\beta}t_\alpha^\dagger t_\beta^\dagger\left|0\right\rangle. \end{aligned}$$

Therefore using similar reasoning as the singlet channel the Born amplitude of the triplet channel with polarisation μ is given by,

$$M_\mu^{(1)} = \frac{1}{2}\epsilon_{\mu\alpha\beta}\epsilon_{\mu\gamma\delta}M_{\alpha\beta,\gamma\delta}.$$

Also we have that $P^2 = 2$ for the triplet channel.

C.3 Quadrapole Channel, S = 2

The final channel is the quadrupole channel. This channel is more complex than the other two channels and it is difficult to present a general form as in the previous channels. However we can take advantage of a fundamental property of the irreducible representation which says that all three irreducible representations are rotationally invarient, and therefore we can find the Born amplitude for some specific polarisation of the triplons and it will generalise to all polarisation.

Therefore as we have that the quadrupole channel is represented by the symmetric traceless rank 2 tensor,

$$\begin{aligned} S_{\alpha\beta} &= \frac{\left(\tau_{\alpha\beta}+\tau_{\beta\alpha}\right)}{2} - \frac{1}{3}\delta_{\alpha\beta}\tau_{\alpha\beta}, \\ &= \frac{1}{2}\left(\tau_{\alpha\beta}+\tau_{\beta\alpha} - \frac{2}{3}\delta_{\alpha\beta}\tau_{\alpha\beta}\right). \end{aligned}$$

Therefore we can see that choose two different polarisations will greatly simplify the channel. In this case we will take $\alpha = x$ and $\beta = y$ and therefore we are left with,

$$S_{xy} = \frac{1}{2}\left(t_x^\dagger t_y^\dagger + t_y^\dagger t_x^\dagger\right).$$

Therefore the initial normalised wavefunction for this polarisation will be,

$$|\psi_i\rangle = \frac{1}{\sqrt{2}}\psi_i\left(\mathbf{q}\right)\left(t_x^\dagger t_y^\dagger + t_y^\dagger t_x^\dagger\right)\left|0\right\rangle.$$

Therefore the Born amplitude for the quadrupole channel is given by,

$$\begin{aligned} M^{(2)}(\mathbf{q},\mathbf{p}) &= \langle \psi_f \,|\, M_{\alpha\beta,\gamma\delta} \,|\, \psi_i \rangle \,, \\ &= \frac{1}{2} \left(\delta_{x\gamma}\delta_{y\delta} + \delta_{x\delta}\delta_{y\gamma}\right) M_{\alpha\beta,\gamma\delta} \left(\delta_{x\alpha}\delta_{y\beta} + \delta_{x\beta}\delta_{y\alpha}\right). \end{aligned}$$

Appendix D

Numerical Calculations

The numerical calculations used in this thesis are trivial however for the sake of self containment I feel it necessary to give a brief overview of the methods used. All numerical calculations were completed in the c programming language and due to their simplicity require no deep understanding. In the calculation of the non analytic integrals in chapter 3 we converted them to their summation form and then perform the sum over 10000 evenly spaced points in a $2\pi \times 2\pi$ grid. For the root finding component of the program we use a simple "if" function to test whether the absolute value of each subsequent value is less than the absolute of the point before it. A sample code for "Binding energy vs Coupling constant" for the singlet channel $\mathbf{Q} = 0$ case is provided below.

```
// Bryce Lackenby 28/05/2014.
// Bound State of Triplons Thesis Semester 1 2014.
// This code will print the unitless binding energy of a triplon for
// each coupling constant ratio.


#include <stdlib.h>
#include<stdio.h>
#include <math.h>

// Definition of constants in code. ITERATIONS is the number of point taken
// between -PI and PI and RESOLUTION is the resolution of the final plot
// and binding energies tested
#define ITERATIONS 100
#define BOUNDARY   6.283185307
#define RESOLUTION 0.001
#define PI         3.14159265359

// Functions
double FUNCTION(double x, double y, double a, double k);

int main(int argc, char *argv[]) {
```

```
// Declaration of variables
double counterx;
double countery;
double interval;
double b;
double sum = 0;
double root = -20;
double rootvalue = 2;
double k;

// creates and points to a file to write data to.
FILE *fp;
fp = fopen("SingletCoupling.dat", "w");

// Loops over each value for the coupling constant.
for(k = 0.9; k <= 7 ; k = k + RESOLUTION) {

    //Loops over binding energies.
    for(b = 0; b <= 2; b = b + RESOLUTION) {
        //Following two loops finding the value of the sum of the
        //function in the 2PI*2PI grid.
        for(counterx = -PI + 0.0001; counterx < PI ;
            counterx = counterx + interval){
            for(countery = -PI + 0.0001; countery < PI;
                countery = countery + interval){
                sum = sum + FUNCTION(counterx, countery, b, k);
            }
        }

            // Root finding equation.
            if(fabs(sum) < fabs(root)){
                root = sum;
                rootvalue = b;
            }
            else{}

            // Reinitialises sum.
            sum = 0;
    }

    // Prints the value of the coupling constant and corresponding
    // root to the file.
    if(rootvalue != 2){
        fprintf(fp, "%lf, %lf \n", k, rootvalue);
    }

    else{}

    root = -20;
}

fclose(fp);
```

```
    return EXIT_SUCCESS;
}

//Function that needs to be summed in the region. In this case it is the
//singlet condition
double FUNCTION(double x, double y, double a, double k) {

    double ANSWER;

    ANSWER = (1/k + 0.5*(cos(x) + cos(y)))/((a + 4 + 2*cos(x) + 2*cos(y)));

    return ANSWER;

}
```

All numerical calculations use this method when finding the summation in the Brillouin zone.

Bibliography

[1] L.D. Landau. Theory of the Superfluidity of Helium II. *Physical Review*, 60(4), 1941.

[2] S.N. Bose. Plancks Gesetz und Lichtquantenhypothese. *Zeitschrift für Physik*, 26(178), 1924.

[3] A. Einstein. Quantentheorie des einatomigen idealen Gases. *Sitzungsberichte der Preussischen Akademie der Wissenschaften*, 1(3), 1925.

[4] J. Bardeen, L. N. Cooper, and J. R. Schreiffer. Microscopic Theory of SuperConductivity. *Physical Review*, 106(162):3, 1957.

[5] D.C. Mattis. *The Theory of Magnetism*. Springer, 1965.

[6] J.G. Bednorz and K.A. Mueller. Possible high TC superconductivity in the Ba-La-Cu-O system. *Zeitschrift für Physik B*, 64, 1986.

[7] J.G. Bednorz and K.A. Mueller. PEROVSKITE-TYPE OXIDES - THE NEW APPROACH TO HIGH-Tc SUPERCONDUCTIVITY. In *Nobel lecture*, 1987.

[8] A.J. Leggett. What do we know about HT_c? *Nature Physics*, 2, 2006.

[9] C.Q Choi. Iron Exposed as High-Temperature Superconductor: Scientific American. *Scientific American*, 2008.

[10] P.W. Anderson. The Resonating Valence Bond State in La2CuO4 and Superconductivity. *Science*, 235(4793), 1987.

[11] L. Balents. Spin liquids in frustrated magnets. *Nature*, 464, 2010.

[12] J.R. Schrieffer and J.S. Brooks, editors. *Handbook of High-Temperature Superconductivity*. Springer Science, 1 edition, 2007.

[13] P.W. Anderson. RESONATING VALENCE BONDS: A NEW KIND OF INSULATOR? *Materials Research Bulletin*, 8, 1973.

[14] X.G. Wen. Quantum Orders and Symmetric Spin Liquids. *Physical Review B*, 65(165113), 2002.

[15] John Micheal Ziman. *Theory of Solids*. Cambridge University Press, Cambridge, 2 edition, 1972.

[16] N.W. Ashcroft and N.D. Mermin. *Solid State Physics*. Saunders College, 1 edition, 1976.

[17] G.F. Newell and E.W. Montroll. On the Theory of the Ising Model of Ferromagnetism. *Reviews of Modern Physics*, 25(2), 1953.

[18] C.G. Shull, W.A. Strauser, and E.O. Wollan. Neutron Diffraction by Paramagnetic and Antiferromagnetic Substances. *Physical Review*, 83(2), 1951.

[19] C.G. Shull. Detection of Antiferromagnetism by Neutron Diffraction. *Physical Review*, 76(1256), 1949.

[20] M. Greven. *Neutron Scattering Study of Magnetism in Insulating and Superconducting Lamellar Copper Oxides*. PhD thesis, M.I.T., 1995.

[21] L.D. Landau. Properties of metals at very low temperatures. *Zh. Eksp. Teor. Fiz.*, 7(379), 1937.

[22] N.D. Mermin. Crystalline Order in Two Dimensions. *Physical Review*, 176(1), 1968.

[23] Sidney Coleman. *Aspects of Symmetry*. Cambridge University Press, 1 edition, 1985.

[24] J. Goldstone. No Title. *Nuovo Cimento*, 19(154), 1961.

[25] E. M. Lifshitz and L. P. Pitaevskii. *Course of Theoretical Physics: Volume 9, Statistical Physics, Part 2*. Pergamon Press, New York, 3 edition, 1991.

[26] Alexander Atland and Ben Simons. *Condensed Matter Field Theory*. Cambridge University Press, New York, 2nd edition, 2010.

[27] J. Van Kranendonk and J. H Van Klack. Spin Waves. *Reviews of Modern Physics*, 30(1):22, 1958.

[28] J. Zinn-Justin. *Quantum Field Theory and Critical Phenomena*. Clarendon Press, Oxford, 3rd edition, 1996.

[29] A.W. Sandvik, A.V. Chubukov, and S. Sachdev. Quantum critical behaviour in a two-layer antiferromagnet. *Physical Review B*, 51(22), 1995.

[30] S Sachdev. *Quantum Phase Transitions*. Cambridge University Press, 2 edition, 2011.

[31] S. Sachdev and B. Keimer. Quantum Criticality. 2011.

[32] N.D. Mermin and H. Wagner. ABSENCE OF FERROMAGNETISM OR ANTIFERROMAGNETISM IN ONE- OR TWO-DIMENSIONAL ISOTROPIC HEISENBERG MODELS. 17(22):1133–1136, 1966.

[33] L.D. Landau and E.M. Lifshitz. *Statistical Physics, Part 1*. Elsevier, Oxford, 3rd edition, 1980.

[34] D.J. Thouless. Long-Range Order in One-Dimensional Ising Systems. *Physical Review*, 187(2), 1969.

[35] A.V. Chubukov. Phase transitions, longnitudinal spin fluctuations, and scaling in a two-layer antiferromagnet. *Physical Review B*, 52(5), 1995.

[36] M.P. Gelfand, R.R.P. Singh, and D.A. Huse. Zero temperature ordering in a two-dimesional frustrated antiferromegnet. *Physical Review B*, 40(16), 1989.

[37] P. Shevchenko, a. Sandvik, and O. Sushkov. Double-layer Heisenberg antiferromagnet at finite temperature: Brueckner theory and quantum Monte Carlo simulations. *Physical Review B*, 61(5):3475–3487, February 2000.

[38] A. N. Vasil'ev, M. M. Markina, and E. A. Popova. Spin gap in low-dimensional magnets (Review). *Low Temperature Physics*, 31(3-4), 2005.

[39] S. Sachdev and R. N. Bhatt. Bond-operator representation of quantum spins: Mean-field theory of frustrated quatum Heisenberg antiferromegnets. *Physical Review B*, 41(9323):7, 1990.

[40] V. Kotov, O. Sushkov, Zheng Weihong, and J. Oitmaa. Novel Approach to Description of Spin-Liquid Phases in Low-Dimensional Quantum Antiferromagnets. *Physical Review Letters*, 80(26):5790–5793, June 1998.

[41] N.N. Bogoliubov. Dubna Report (Unpublished). Technical report, 1962.

[42] H. Wagner. No Title. *Z. Physik*, 195(273), 1966.

[43] S Sachdev. Quantum magnetism and criticality. *Nature Physics*, 4(173), 2008.

[44] A.J. Millis and H. Monien. Spin Gaps and Spin Dynamics in La_{2-x}Sr_xCuO_4 and YBa_2Cu_3O_{7- \delta}. *Physical Review Letters*, 70(18), 1993.

[45] B Normand and Tm Rice. Electronic and magnetic structure of LaCuO2.5. *Physical review. B, Condensed matter*, 54(10):7180–7188, September 1996.

[46] S. Gopalan, T.M. Rice, and M. Sigrist. Spin ladders with spin gaps: A description of a class of cuprates. *Physical Review B*, 49(13), 1994.

[47] A.V. Dotsenko. Effective action approach to a bi-layer frustrated antiferromagnet. 1995.

[48] Kazuo Hida. Dimer Expansion Study of the Bilayer Square Lattice Frustrated Quantum Heisenberg Antiferromagnet. 2013.

[49] E. E. Salpeter and H. A. Bethe. A Relativistic Equation for Bound State Problems. *Physical Review*, 84(6), 1951.

[50] V.B. Berestetskii, E.M. Lifshitz, and L.P. Pitaevskii. *Qauntum Electrodynamics*. Pergamon Press, 2nd edition, 1971.

[51] O.P. Sushkov and V.N Kotov. Bound States of Magnons in the S = 1/2 Quantum Spin Ladder. *Physical Review Letters*, 81(9), 1998.

[52] L.D. Landau and E.M. Lifshitz. *Quantum Mechanics (Non-Relativistic Theory)*, volume 3. Pergamon Press Ltd., volume 3 edition, 1977.

[53] V.E. Demidov, O. Dzyapko, S.O. Demokritov, G.A. Melkov, and A.N. Slavin. Observation of Spontaneous Coherence in Bose-Einstein Condensate of Magnons. *Physical Review Letters*, 100(047205), 2008.

[54] Y.D. Kalafati and V.L. Safonov. Possibility of Bose condensation of magnons excited by incoherent pump. *Pis'ma Zh. Eksp. Teor. Fiz.*, 50(3), 1989.

[55] V. Zapf, M. Jaime, and C.D. Batista. Bose-Einstein condensation in quantum magnets. *2Reviews of Modern Physics*, 86, 14.

[56] J.J. Sakurai and J.J. Napolitano. *Modern Quantum Mechanics*. Pearson, 2 edition, 2011.